nature electronics

Article

https://doi.org/10.1038/s41928-025-01411-4

Measurements of redox balance along the gut using a miniaturized ingestible sensor

Received: 18 October 2024

Accepted: 8 June 2025

Published online: 16 July 2025

Check for updates

Aniek Even[1,2,8] ✉, Roseanne Minderhoud[1,3,4,5,8], Tom Torfs[6], Francesca Leonardi[1,2], Arjan van Heusden[1,2], Ria Sijabat[1,2], Dimitrios Firfilionis[1,2], Ivan Dario Castro Miller[6], Ramzy Rammouz[6], Tobias Teichmann[1,2], Ruben van Bergen[1,2], Günter Vermeeren[7], Edoardo Capuano[1,4], Rachel Armstrong[1,2], Klaus Mathwig[1,2], Sonja de Vries[1,5], Annelies Goris[1,2], Nick Van Helleputte[6], Guido Hooiveld[1,3] & Chris Van Hoof[1,2,6]

Redox balance—the equilibrium between oxidants and reductants—is a key modulator of a healthy gut and consequently overall well-being. Excess reactive species, resulting in oxidative stress, are linked to deleterious processes including inflammation and microbiome dysbiosis. However, a lack of suitable in vivo methods has restricted measurements of redox balance in the human gut. Here we report a miniaturized ingestible sensor that is equipped with an oxidation–reduction potential sensor, an electrochemical reference electrode and pH and temperature sensors. We preclinically validate our wireless gastrointestinal (GI) smart module (GISMO) in GI fluids and an animal model and report in-human measurements in 15 healthy individuals. Our high-temporal-resolution data, measured every 20 s, reveal consistent profiles from an oxidative environment in the stomach to a strongly reducing environment in the large intestine. This non-intrusive method has the potential to advance (GI) disease monitoring and offer insights into the gut microbiome.

The gastrointestinal (GI) barrier plays a crucial role in maintaining gut health and, consequently, overall homeostasis. It balances the absorption of essential nutrients and water while preventing entry of harmful foreign substances and pathogens. This balance is facilitated by cooperation between the host, immune system and gut microbiota[1]. A key modulator and important signalling mechanism is redox balance[2]. Although redox state has not generally received levels of recognition similar to pH, the transfer of electrons in redox reactions is equally vital to living organisms as the transfer of protons in acid–base reactions[3]. Disturbances in redox biology can lead to oxidative stress—an imbalance between oxidants and antioxidants[4]—which has been associated with several diseases and disorders including inflammatory bowel disease (IBD)[5], microbiome dysbiosis[6], GI cancers[7] and even early death in animal models[8].

Direct measurements of redox balance are feasible with an oxidation–reduction potential (ORP) sensor. When exposed to a solution, the voltage difference between a working electrode and reference electrode (RE) is a direct measurement of redox potential. A positive ORP value indicates an oxidizing environment; a negative potential indicates a reducing environment. Although ORP sensors are commonly used in some disciplines (such as water and soil measurements[3]), in vivo measurements have only been performed in rodents[9,10]. Attempts to

[1]OnePlanet Research Center, Wageningen, the Netherlands. [2]imec, Wageningen, the Netherlands. [3]Division of Human Nutrition and Health, Wageningen University & Research, Wageningen, the Netherlands. [4]Food Quality and Design Group, Wageningen University & Research, Wageningen, the Netherlands. [5]Animal Nutrition Group, Wageningen University & Research, Wageningen, the Netherlands. [6]imec, Leuven, Belgium. [7]Department of Information Technology, Ghent University, Ghent, Belgium. [8]These authors contributed equally: Aniek Even, Roseanne Minderhoud.
✉e-mail: aniek.even@imec.nl

https://doi.org/10.1038/s41928-025-01411-4

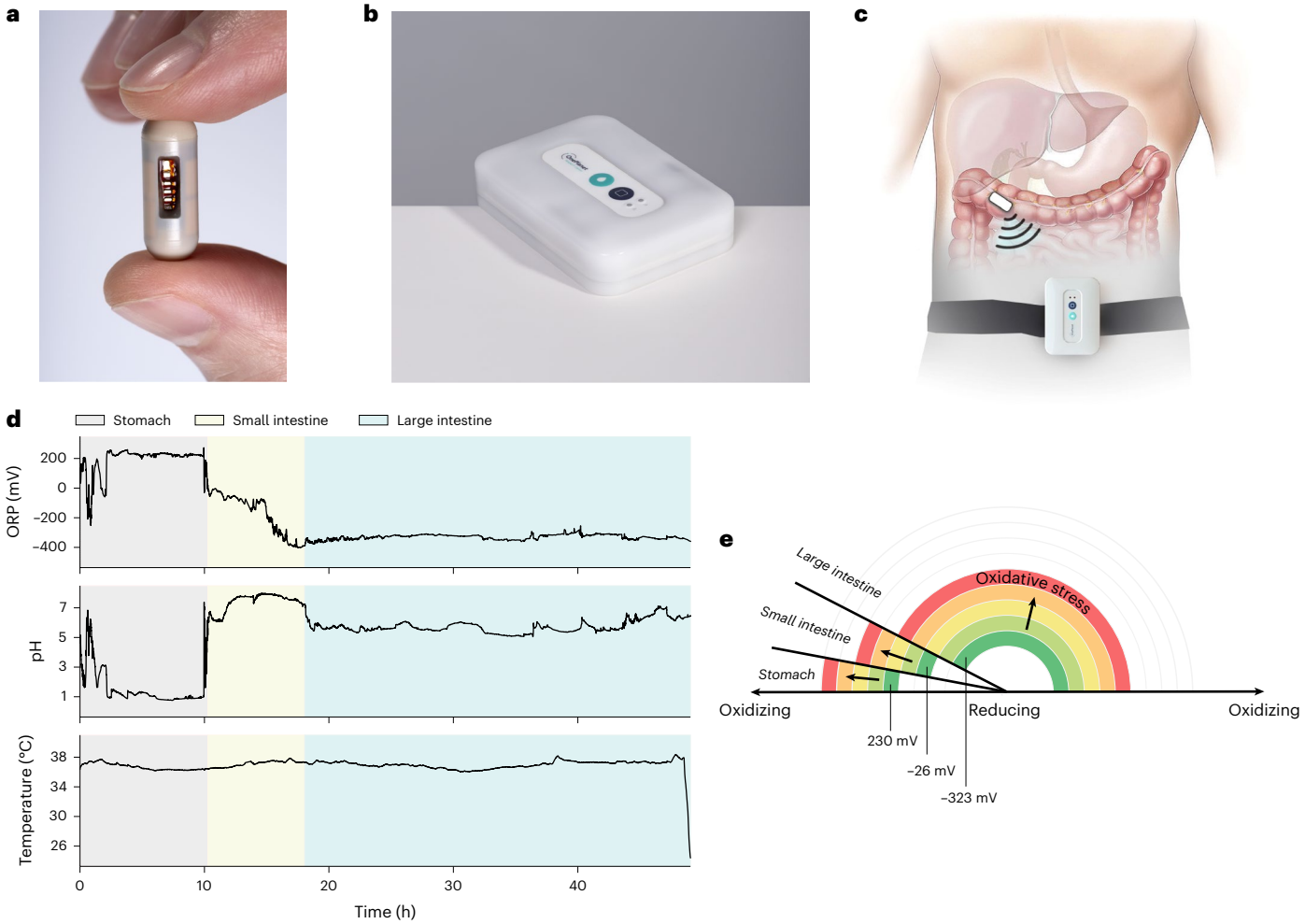

Fig. 1 | GISMO ingestible system overview and example data of in-human redox balance measurements along the gut. a, The miniaturized ingestible sensor capsule (length 21 mm; diameter 7.5 mm) measures redox balance (ORP), pH and temperature. **b**, Data are sent wirelessly to a compact wearable receiver worn outside the body. **c**, Schematic illustration of the full system in operation. **d**, Example data from our human trial show distinct GI regions. The redox environment (top) is strongly oxidizing in the stomach, slightly reducing in the small intestine and highly reducing in the large intestine. pH values (middle) were measured simultaneously. Temperature (bottom) was used to confirm body exit. **e**, We acquired gut redox reference values in 15 healthy participants from a total of 66 ingestibles. The redox values in these healthy volunteers rarely exceeded 230 mV in the stomach, −26 mV in the small intestine or −323 mV in the large intestine (95th-percentile values across all measurements). In a disturbed gut environment, for example due to inflammation or microbiome dysbiosis, an imbalance between oxidants and antioxidants can occur, leading to an excess of reactive species and resulting in oxidative stress. This shift to a more oxidative environment is indicated by the arrows, moving from the healthy region in green (baseline values differ per segment) towards the oxidative stress region in red. The size of the illustrated segments corresponds to the average regional transit times: 4.1 h for the stomach, 6.2 h for the small intestine and 57.3 h for the large intestine. Image in **c** from Pixabay.

measure ORP in humans have been limited to faecal analysis, which were deemed unsuitable for discriminating between patients and healthy controls[11], most likely due to the highly reactive nature of oxidants and the effect of oxygen in the environment. Other clinical studies have resorted to indirect indicators of oxidative stress, such as oxidative damage to DNA, lipids and proteins, or antioxidant status. These approaches measure the damage caused by oxidative stress but do not directly capture the dynamic nature of the process[12–14].

Performing direct measurements in the human GI tract is challenging due to its complexity and inaccessible nature. Common clinical tools (such as upper endoscopy and colonoscopy), which offer visual inspection but are invasive, cannot assess the entire GI tract and lack sensitivity to oxidative stress[15]. Wireless capsule endoscopies[16,17] do facilitate inspection of the small intestine. However, they are equally unsuited for direct redox measurements due to the lack of embedded sensors and the need for bowel preparation, which alters the gut environment[18]. Capsules with embedded biochemical sensing have been developed but lack sensors beyond pH[19,20], blood detection[21] and fermentation gases[22,23], and those with additional sensors have not been applied in a clinical setting[24–27].

In this Article, we report a miniaturized (length 21 mm, diameter 7.5 mm), low-power, wireless GI smart module (GISMO). The capsule is equipped with an ORP sensor, a custom electrochemical RE and sensors for pH and temperature. Designed to be ingested orally and to wirelessly communicate with a wearable receiver, it can record along the entire GI tract without requiring special bowel preparation. We report in vitro validation and in vivo validation in an animal model as well as results from 15 healthy volunteers.

Miniature ingestible sensor capsule design

To measure redox balance and pH, the GISMO ingestible system uses a series of electrochemical sensors, as illustrated in Fig. 1. These sensors are integrated into a wireless ingestible capsule together with custom electronics for time-multiplexed sensor readout and wireless

https://doi.org/10.1038/s41928-025-01411-4

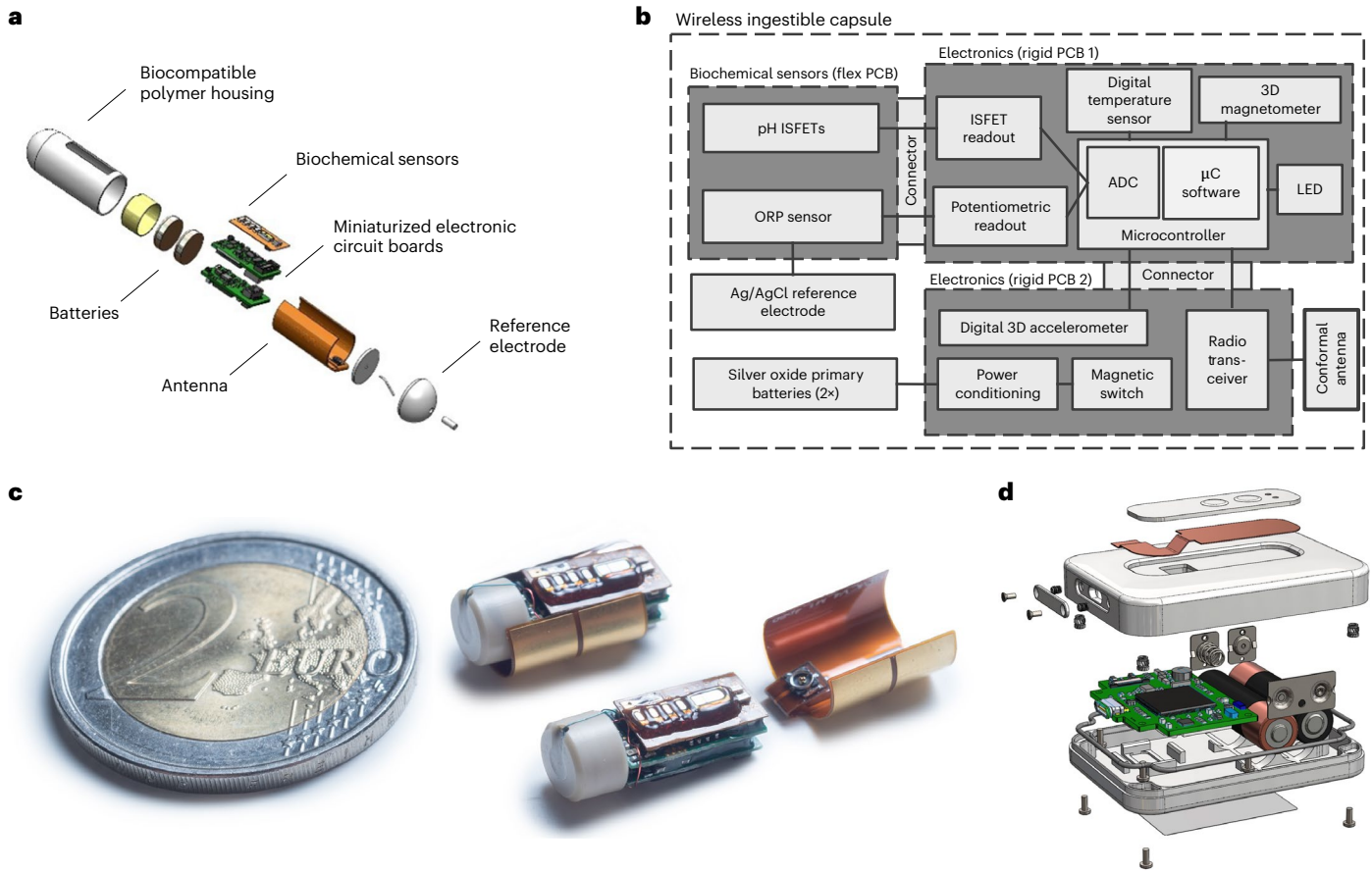

Fig. 2 | GISMO device and wearable receiver architecture and characterization. **a**, Exploded view of the ingestible including electrochemical sensors, electronics, conformal antenna, batteries and RE in a PEEK biocompatible housing. **b**, Block diagram of the main parts of the ingestible subdivided in two thin rigid PCBs, a flexible (flex) PCB with the electrochemical sensors, the RE, batteries and conformal antenna. **c**, Stacked rigid PCBs and flex PCB together with the battery subassembly and the preshaped conformal antenna, with a 2-euro coin for size comparison. **d**, Exploded view of the wearable battery-operated receiver providing a simple user interface.

communication, a conformal antenna and two silver oxide batteries, all enclosed in a biocompatible polyetheretherketone (PEEK) housing (Fig. 2a). To reduce the risk of retention and facilitate easy ingestion, the capsule is size '0' (21 mm × 7.5 mm), which is three times smaller in volume than capsule endoscopes[28], three times smaller than a commonly used pH capsule[19], 1.7 times smaller than a—not yet clinically validated—inflammation-marker capsule[24] and 2.8 times smaller than a gas-based ingestible sensor[29]. To achieve such aggressive miniaturization, we optimized the volume occupied by all subcomponents.

Although ORP measurements are commonplace in other domains, successfully deploying them in a miniaturized ingestible capsule necessitates development of compact working electrodes and REs. These electrodes need to deliver stable performance throughout the measurement and endure the harsh environment of the GI tract. To this end, we designed a custom chip with a platinum electrode for the ORP sensor. Accurate pH measurement is ensured by two redundant pH sensor chips based on ion-sensitive field-effect transistor technology (ISFET; Sentron). The sensor surfaces are either Pt or chemically inert glass-like oxides and can withstand the acidic environment of the stomach. We custom-designed our RE such that drift remains below 0.06 mV h^{-1}. The reference occupies the entire dome on one side of the capsule (59 mm^3). The dome contains a Ag/AgCl wire immersed in a KCl gel saturated with AgCl. To protect the sensitive electronics inside the capsule from the hostile GI environment, everything is hermetically sealed with epoxy resin such that only the sensor surfaces and RE are exposed. The porous RE frit (thickness 0.4 mm and diameter 1 mm) is designed to ensure an optimal tradeoff between electrical impedance and leakage to the outer environment (Extended Data Fig. 1).

The biochemical sensors are integrated on a flexible printed circuit board (PCB), which is stacked on top of two miniature rigid PCBs containing the electronics (Fig. 2b). The first of these rigid PCBs includes the electrochemical sensor readout, a low-power microcontroller, a high-precision temperature sensor and a three-dimensional (3D) magnetometer. The second PCB includes a power conditioning circuit, a magnetic switch for power-on, a 3D accelerometer and a radio transceiver. The use of low-power electronics, hardware reuse for multisensor readout, aggressive duty-cycling and microcontroller software optimization were key to achieving the desired miniaturization.

To further save volume inside the capsule, we designed a conformal wrap-around antenna. In a tradeoff between antenna size and efficiency on the one hand and path loss through body tissue on the other hand, 868 MHz (EU license-free band for short range devices) was selected as the communication frequency. An overview of the optimal frequencies for different capsule depths and its comparison to relevant license-free available bands in Europe and Americas is shown in Extended Data Fig. 2a. Because commercial antenna modules are designed for operation in air, they perform poorly in-body due to the characteristic impedance mismatch. Hence, we designed our own custom antenna. It is a custom stepped impedance antenna design[30] adapted to the frequency and the shell material (PEEK) of the pill for efficient operation inside the GI tract. The antenna is designed in a 172-µm-thick flexible circuit board (Fig. 2c) wrapped around the

https://doi.org/10.1038/s41928-025-01411-4

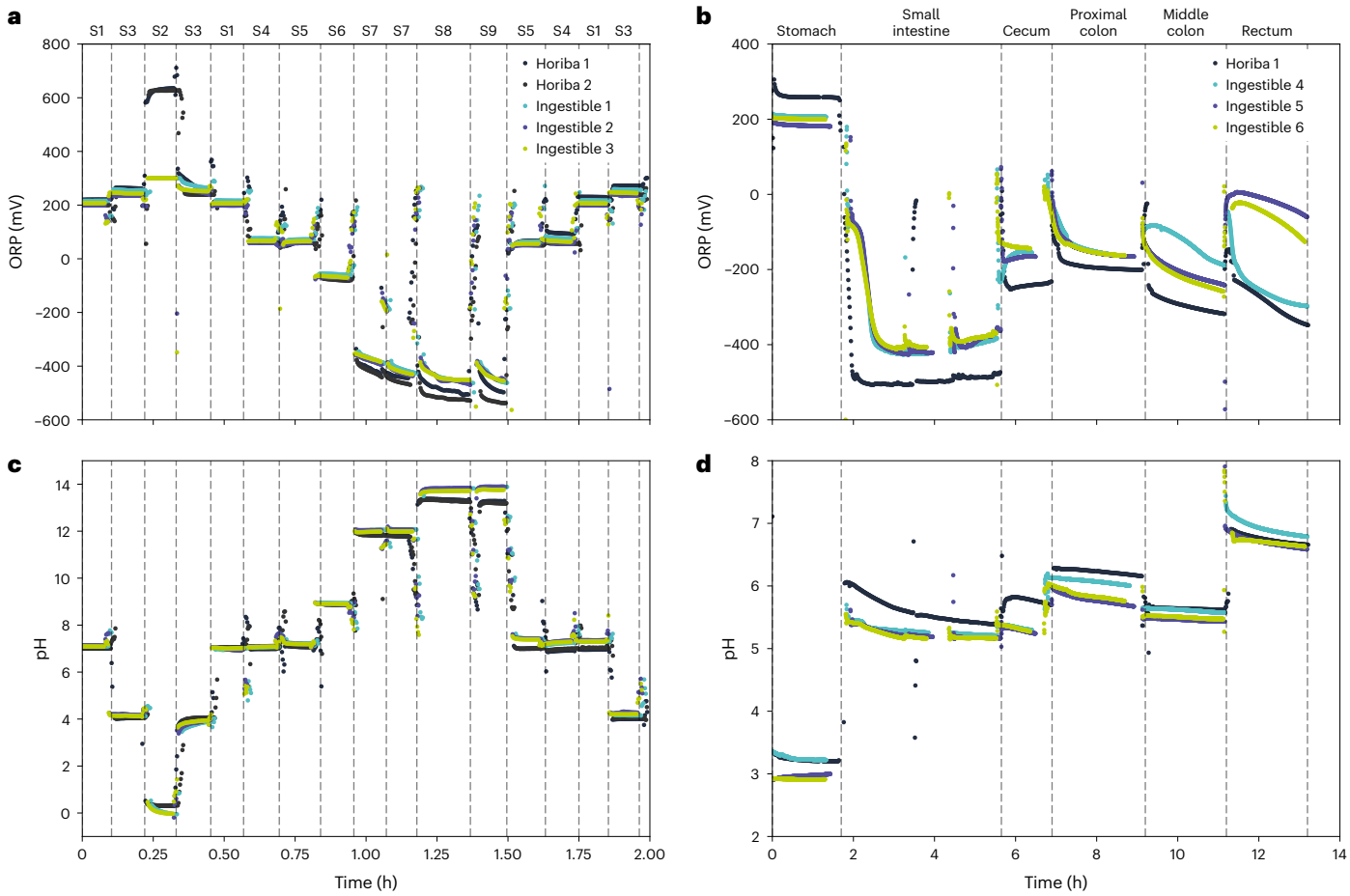

Fig. 3 | In vitro validation of the GISMO sensors. a,**c**, In vitro validation in standard solutions. Staircase measurement of ORP (**a**) and pH (**c**) profiles using three ingestibles show good agreement with two commercial sensors (Horiba) in ORP (alternate) standards in the range of −550 to 280 mV with pH range between 0 and 14. The measurements were performed at body temperature (37 °C) within 2 h due to limited stability of ORP standards prepared in-house by dissolving quinhydrone in pH buffers. For a full description of the solution, see Methods. Note that S2 is out of the designed range of the electronics because ORP values above 280 mV are not expected in the human body. It was challenging to create a highly reducing environment outside the body; for S8 and S9, we observed more variability, as well as between the commercial sensors, possibly due to the extremely high pH and the short lifetime of the solutions. **b**,**d**, To create a more complex and realistic environment, we performed continuous measurement of ORP (**b**) and pH (**d**) in different types of GI fluids collected from a pig post mortem, using three ingestibles versus a commercial sensor (Horiba). Similar trends between the ingestibles and commercial system were observed. The measurements were performed at body temperature (37 °C) and at segment-specific relevant oxygen levels. The ingestibles were briefly taken out of the anaerobic chamber before entering small intestine conditions, which could have caused the time lag with the commercial system because ORP sensors are sensitive to oxygen concentrations.

electronics just inside the encapsulating shell, allowing for optimal use of the volume in the ingestible. This optimization achieved an antenna gain between −33.2 and −20.8 dBi when immersed in a large body phantom of 40 cm diameter. The sensor data are sent in real time wirelessly and encrypted to an unobtrusive wearable receiver (Figs. 1b and 2d).

A pair of compact non-rechargeable silver oxide batteries (SR516SW, nominal capacity 12.5 mAh at a voltage of 1.55 V each) are used to power the capsule. This battery chemistry was selected for its safety and proven use in other ingestible capsules[31]. The batteries were assembled using a combination of wire bonding and conductive epoxy. To ensure sufficiently long shelf life, the entire ingestible is activated by a magnetic reed switch such that the power-off consumption is only 0.13 µA, which discharges the batteries only ~7–8% over a period of six months. In line with typical transit times[32,33], we designed the ingestible to function for at least five days while measuring and transmitting all sensors (temperature, dual pH and ORP) every 20 s, which provides very detailed measurement profiles. The ingestible has an average current consumption of only 28 µA during normal operation (Extended Data Fig. 3). After five days, the ingestible switches to an ultra-low-power mode (9.4 µA average current) where only the temperature and limited housekeeping data are transmitted. The ingestible can operate for at least nine more days (two weeks total) in this mode. This provides an additional safety mechanism to confirm device exit in case of abnormally long transit times. The full functionality, power consumption and battery lifetime were tested in a closed container with physiological saline solution in an oven at 37 °C (Extended Data Fig. 3c).

Extensive electronic testing was performed to validate the electronic readout and communication robustness in representative phantoms (Extended Data Fig. 2b,c).

In vitro sensor validation

To validate the ORP and pH sensors in vitro, we conducted experiments in progressively complex environments, starting with standard solutions of precisely known concentrations and advancing to porcine GI fluids.

For the validation in standard solutions, we used commercially available ORP standards of 220 and 600 mV. Due to limited availability of standards in other mV ranges—negative commercial ORP standards do not exist—additional standard solutions were prepared in-house to generate a range of solutions covering the values anticipated in the GI

tract of −550 to 280 mV (refs. 9,34,35). Figure 3a,c shows recordings of three ingestibles and two commercial systems (Horiba). The measured ORP values show strong consistency between the ingestibles and the commercial ORP sensors. Some variability is observed in the negative ORP solutions, which is also seen between the two commercial systems. This variability is likely attributable to the short lifetime of the solutions and the extreme pH levels (pH 12 and 14). These extremely basic pH conditions are not expected in the GI tract, but they are needed to create such a strongly reducing environment outside the body. The ingestibles system is designed to measure values up to 280 mV because higher values are not anticipated in the GI tract; hence the clipping for the 600-mV solution. The pH sensors can measure in the full pH range (0–14) and are in good agreement with the commercial systems.

To validate the sensors in a more realistic and complex environment, we used GI fluids collected from post mortem pigs placed in a temperature-controlled anaerobic chamber, mimicking gut conditions (Fig. 3b,d). We observed a slight offset between the commercial sensor (Horiba) and our ingestibles and some differences among the three ingestibles in the middle colon and rectum. Nevertheless, the overall trend was similar. Even though these samples are actual GI fluids and the best available method to mimic the gut outside the body, the properties of the GI fluids seem to change over time after thawing. We observed clear phase separation in the sample from the small intestine, which resulted in a lower-than-expected pH. The inhomogeneities in the samples and changing properties could have resulted in some slight variation in measurements. Despite the challenges, we showed that our ingestibles can measure ORP and pH in the relevant range and are in good agreement with a commercial system.

In vivo validation in an animal model

In vivo functionality was validated in live pigs, a commonly used model for the human digestive system[36–38]. One example data trace of ORP, along with supporting pH and temperature data, is given in Fig. 4a. Three different regions of the GI tract can be distinguished: (1) stomach region with ORP values between −50 and 250 mV, (2) small intestine region with ORP values between −250 and −50 mV and (3) large-intestine region with ORP values lower than −300 mV. Our observations align with findings from the limited number of rodent studies, where direct measurements in the caecum of mice and rats have shown similar reducing environments ranging from −320 to −554 mV (refs. 9,10).

Of the nine ingestibles administered, five examples are shown in Fig. 4. Of the other ingestibles, one had only pH sensors, and three stopped prematurely in the stomach (after 22.5 and 25 h, respectively) or in the beginning of the large intestine (after 48.5 h). In four ingestibles, we could not define the entry of the large intestine based on the pH profiles as conventionally used. However, we did observe a notable change in redox values. The example in Fig. 4a shows coinciding starts of the transitions in pH (from 7.9 to 6.0) and ORP (from −100 to −350 mV) going from the small intestine to the large intestine. In contrast, in four ingestibles without a significant pH change at the transition from the small intestine to the large intestine, the ORP dropped from an average 100 mV to −325 mV (Fig. 4b–e). For one of these four sensor capsules, an ultrasound examination was performed 67 h after ingestion (Fig. 4e). The ultrasound scan confirmed that the ingestible was located in the large intestine, as signalled by the low ORP value (−303 mV), which would have been missed based on pH alone.

In-human baseline measurements of redox balance

For the clinical evaluation, we recruited 15 healthy volunteers and planned for each to receive five ingestibles. Because this was the first time these were used in humans, the initial phase of the study focused on validating safety and reliable operation. Participants received one GISMO capsule in the morning, after an overnight fast. All participants comfortably ingested the capsule, which passed through their bodies without issues or discomfort, and no abnormal effects were observed. All capsules successfully recorded data and transmitted data reliably. After all participants agreed to continue, phase 2 of the clinical evaluation commenced two months later. In this phase, the volunteers received one morning and one evening pill on two separate days spread over two weeks. The morning ingestibles were given after an overnight fast; the evening ingestibles were given just before the evening meal. In total, 69 ingestibles were administered over both phases combined, of which 66 (Methods) were used in the subsequent analyses. The ingestible sensors were calibrated pre-ingestion, for interpretation of the GI data, and post-excretion, for sensor performance and drift characterization. Throughout the trial, we observed robust wireless communication. During nighttime use, participants placed the wearable receiver and an additional non-wearable receiver next to their bed. Participants were allowed to remove the wearable receiver for short durations (for example, during showering or light-intensity sports). Despite this, we still achieved overall data coverage (that is, percentage of correctly received data packets) of 90.3% (range 59.1% to 98.9% across all ingestibles). Excluding the period when one of the wearable devices malfunctioned due to being dropped by the participant, the overall data coverage increased to 90.8%, with a range of 71.5–98.9% across all ingestibles. Remaining coverage variability is expected to be caused by factors such as personal habits (for example, relative placement of recording devices at night, removing the device for showering or performing sports), because an evaluation of body mass index (BMI) against coverage did not show a significant correlation. It is worth noting that the data from the ingestible with the receiver malfunction remain relevant and representative of the entire GI tract, as the time when there was no wearable receiver available is sparsely covered by data received from the non-wearable receiver and data recovered from the memory flash of the device. In general, data gaps were rather evenly distributed over the GI tract. The most typical gap size (mode as well as median of the distribution) in our data was a single missed measurement, whereas the 95th and 99th percentile gap sizes were 2.9 and 8.5 min, respectively. A total of 14 gaps were longer than 1 h, with a maximum of 2.5 h. Three ingestibles showed premature battery failure: subsequent investigation showed that this was due to a suboptimal conductive epoxy assembly step, and this assembly step was further optimized to avoid similar premature battery failures in future devices.

We obtained high-temporal resolution sensor data, measured every 20 s. Figure 5 shows resulting pH and ORP traces. The different GI segments were annotated based on significant changes in pH recordings in accordance with generally accepted thresholds (Methods). Temperature readings were used to confirm pill exit (Fig. 1d). Combined data from all analysed ingestibles are shown in Fig. 5a. To account for vastly varying transit times between individuals (Extended Data Table 1), we rescaled the time-series data to physiological regions, making data visualization and interpretation across ingestibles more intuitive (Methods). We found mean (± s.d.) pH values of 2.6 (±1.6) in the stomach, 7.4 (±0.3) in the small intestine and 6.5 (±0.6) in the large intestine. ORP values decreased over the course of the GI tract, starting with an oxidative environment in the stomach (162 ± 70 mV), a slightly reducing state in the small intestine (−126 ± 60 mV) and a strongly reducing environment in the large intestine (−360 ± 16 mV). This is to be expected because there is a strong gradient of decreasing oxygen concentration and increasing microbial activity along the gut[39], both of which influence redox potential. Our unique biochemical characterization of the healthy human gut can serve as a reference for future patient studies, with redox values rarely exceeding 230 mV in the stomach, −26 mV in the small intestine or −323 mV in the large intestine (95th-percentile values across all measurements), as shown in Fig. 1e. In a disrupted gut, we anticipate that these values will increase, shifting towards a more oxidative state.

Although the average pH and ORP signals across the 66 ingestibles display a characteristic profile in which different GI regions can be

https://doi.org/10.1038/s41928-025-01411-4

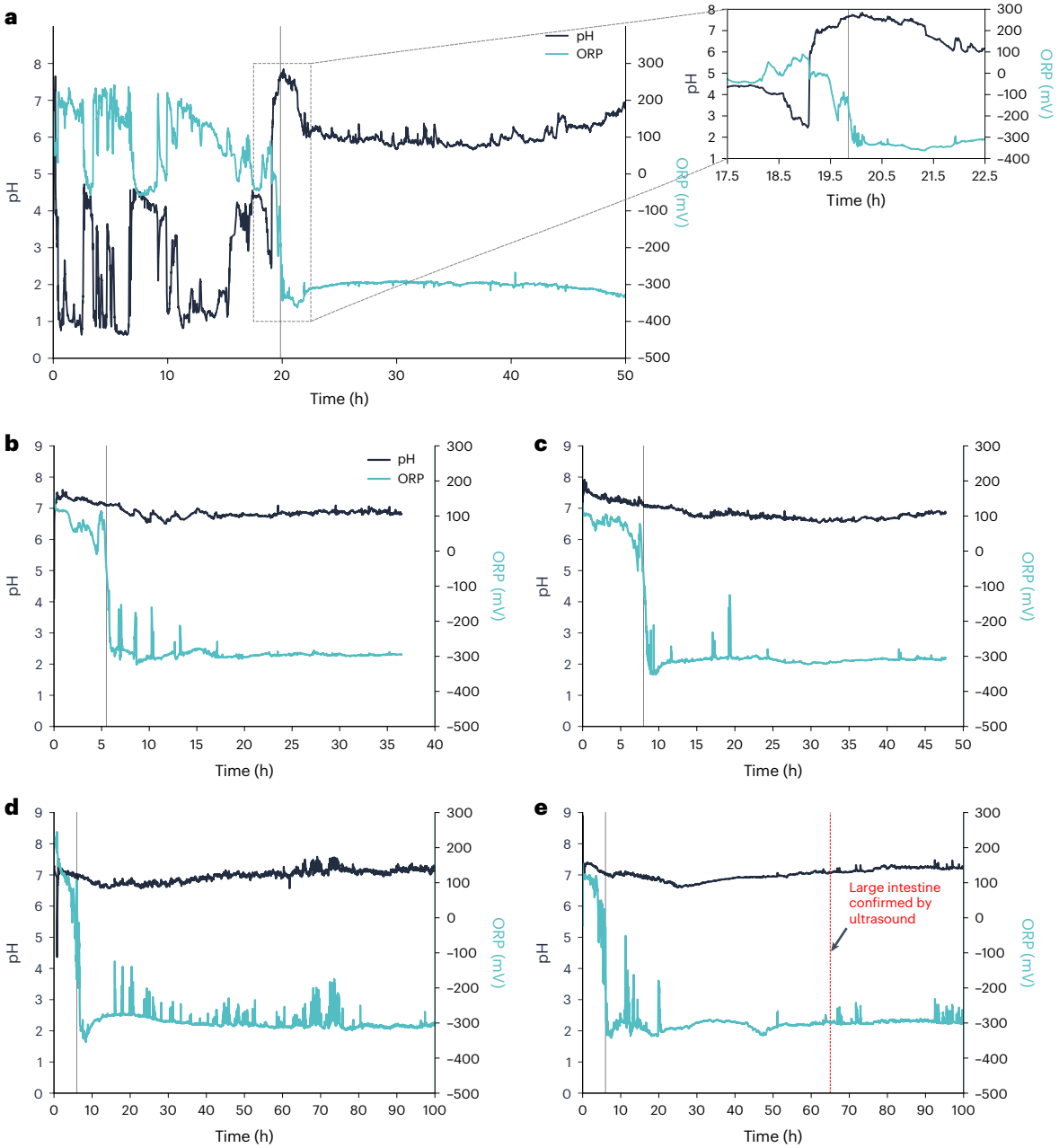

Fig. 4 | In vivo validation of the GISMO ingestible sensor in pigs. a, Measured ORP (mV) and pH profiles along the pig's gut. A zoom-in is provided of the small intestine–large intestine transition. The vertical lines indicate the stomach–small intestine and small intestine–large intestine transition based on combined pH and ORP data. **b**–**e**, Sensor readings of an ingestible showing no distinct small intestine–large intestine transition in pH data, but it was evident in the ORP data. The vertical line indicates entry into the large intestine based on the ORP data. The ingestible was rapidly emptied from the stomach; hence, there is only one transition line. **c,** An ingestible with a very comparable profile to **b**. **d**, Another example where ORP could aid localization. **e,** Similar profile as **b**–**d**. For this ingestible, an ultrasound was performed after 67 h confirming that the ingestible was in the large intestine, as signalled by the ORP data.

clearly distinguished, individual pH and ORP signals displayed substantial variability; examples are shown in Fig. 5c–f (see also Extended Data Figs. 4, 5 and 6). Most often, the ORP signal was stable across most of the small intestine before dropping steeply upon entering the large intestine (Fig. 5c). In other cases, the ORP signal decreased in two distinct steps within the small intestine, potentially corresponding to the jejunum and ileum section (Fig. 4d). In the remaining cases, the ORP decreased more gradually (Fig. 4e) or the decline occurred much earlier in the small intestine (Fig. 5f; see also Extended Data Fig. 5 for a more extensive characterization of the range of ORP profiles observed in the small intestine and Extended Data Fig. 6 for the pH profiles). This variability in the ORP signal appeared to be consistent within participants; there was a significant difference among participants in the relative timing of the pH and ORP drops around the transition into the large intestine (Kruskal–Wallis test; $H(12) = 26.8$, $P = 0.008$, $\eta^2 = 0.31$). This suggests that the timing of these events may reflect some stable physiological or anatomical properties that vary between individuals.

A comparison between the ingestibles administered in the morning on an empty stomach and those taken in the evening shortly after a meal is depicted in Fig. 5b. The pH signal in the stomach fluctuates strongly depending on stomach contents. The pH dips significantly lower for the evening ingestibles ($P = 9.999 \times 10^{-5}$; cluster-based permutation test), which has been described previously[40]. pH signals also diverge significantly in the small intestine, rising to a higher

https://doi.org/10.1038/s41928-025-01411-4

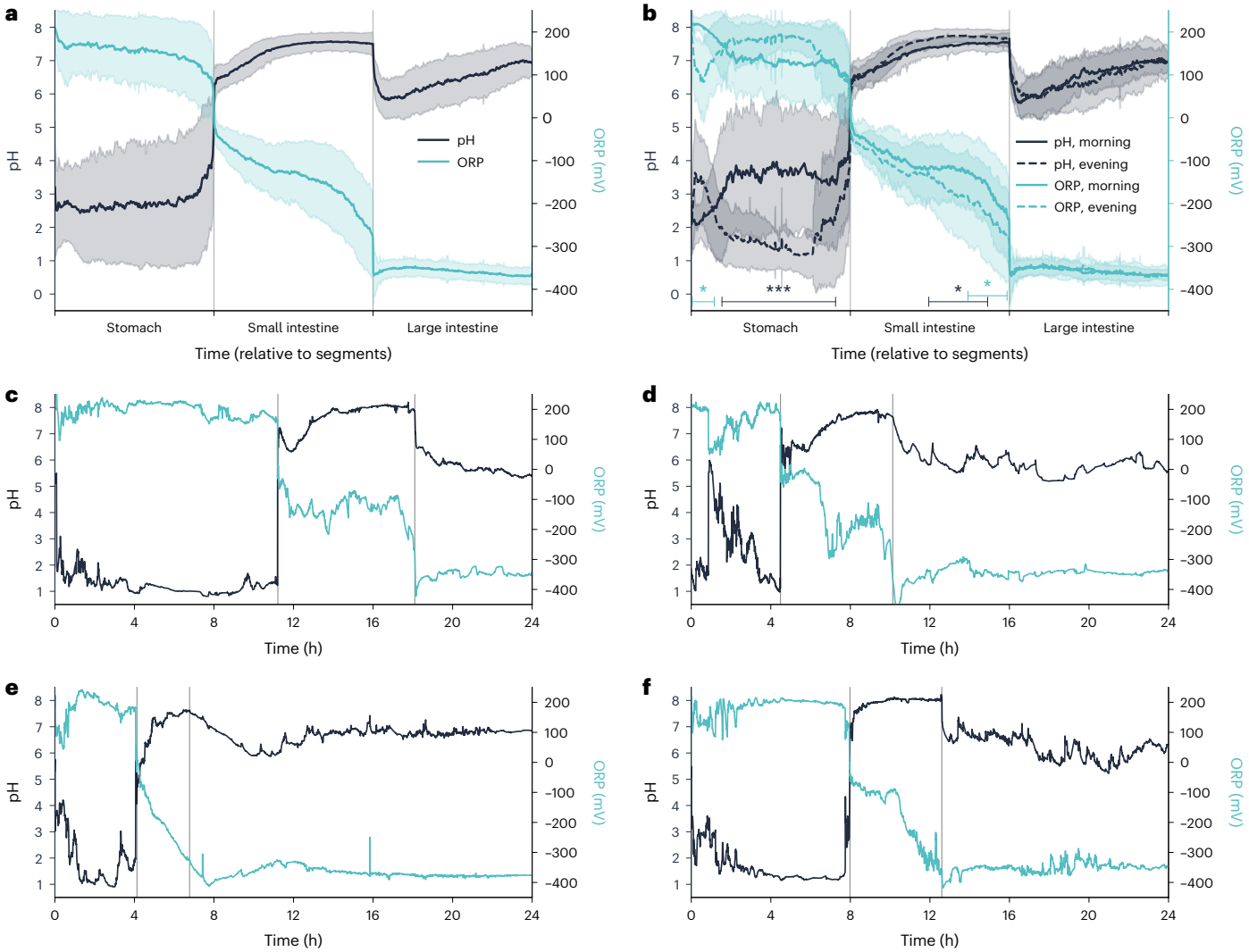

Fig. 5 | Characterization of pH and redox (ORP) measurements along the human GI tract. a, Average pH and ORP recordings of all 66 pills analysed, ingested by 15 participants, linearly rescaled to equal-length compartments (stomach, small intestine and large intestine). Shaded error margins indicate the mean ± 1 s.d. across ingestibles. **b**, As in **a**, but with data from phase 2 of the experiment only, split into ingestibles swallowed in the morning (on an empty stomach; $n = 26$) compared to ingestibles swallowed in the evening (shortly before a meal; $n = 25$). Whiskered horizontal lines at the bottom indicate clusters of contiguous time points that were found to be significantly different between morning and evening pills in a cluster-based permutation test ($N = 10{,}000$ permutations; $^{*}P < 0.05$, $^{***}P < 0.0001$; cluster P values, from left to right: $P = 0.047$, $P = 9.999 \times 10^{-5}$, $P = 0.023$, $P = 0.043$; all P values are two-tailed). **c**–**f**, Illustrative examples of different ORP profiles (along with pH signals from the same ingestibles) observed across the experiment without rescaling to physiological regions. For clarity of exposition, only the first 24 h of data are shown. Vertical lines indicate the (manually annotated) times of small- and large-intestine entry. **c**, The most common profile, consisting of two sharp drops coinciding with the ingestible's entry into the small and large intestine, as identified based on pH. **d**, An example in which the ORP profile shows an additional, intermediate step drop in the small intestine. **e**, An example in which the ORP profile shows a gradual decrease in the small intestine instead of a sharp drop. **f**, ORP profile where the drop in the small intestine is initiated substantially earlier (about halfway through the small intestine) than the drop in pH.

level in the evening ingestibles ($P = 0.023$). Similarly, the ORP signal differs significantly between morning and evening ingestibles in the distal small intestine ($P = 0.043$) as well as for a brief period in the stomach ($P = 0.047$).

Redox measurements to improve ingestible localization

Knowing the GI segment in which the ingestible is located is key to assessing regional transit times in patients with motility disorders, to correlate biomarker measurements to specific gut segments (for example, to locate inflammation) and to guide drug-release or sampling capsules. Although pH measurements are generally accepted for segmentation, the transition between small and large intestine can be difficult to pinpoint[33]. This is corroborated in both our animal study and our clinical trial, in which we observed cases of challenging GI segment annotation based on pH alone, but when combined with ORP, distinct gut regions could be discriminated. Figure 6a shows an example in which clear segmentation based on either pH or ORP is possible, because they drop at the same time. In other cases, the ORP measurement showed a significant change in redox environment, although a clear transition in pH was absent (Fig. 6b,c). We note that in the majority of ingestibles, the ORP drop was observed before the pH drop, and in most other cases they occurred simultaneously. This is in line with a scintigraphy study following the location of a radiolabeled wireless motility capsule while recording pH values, which noted that ingestibles pass the ileal–caecal junction before the pH signal starts

https://doi.org/10.1038/s41928-025-01411-4

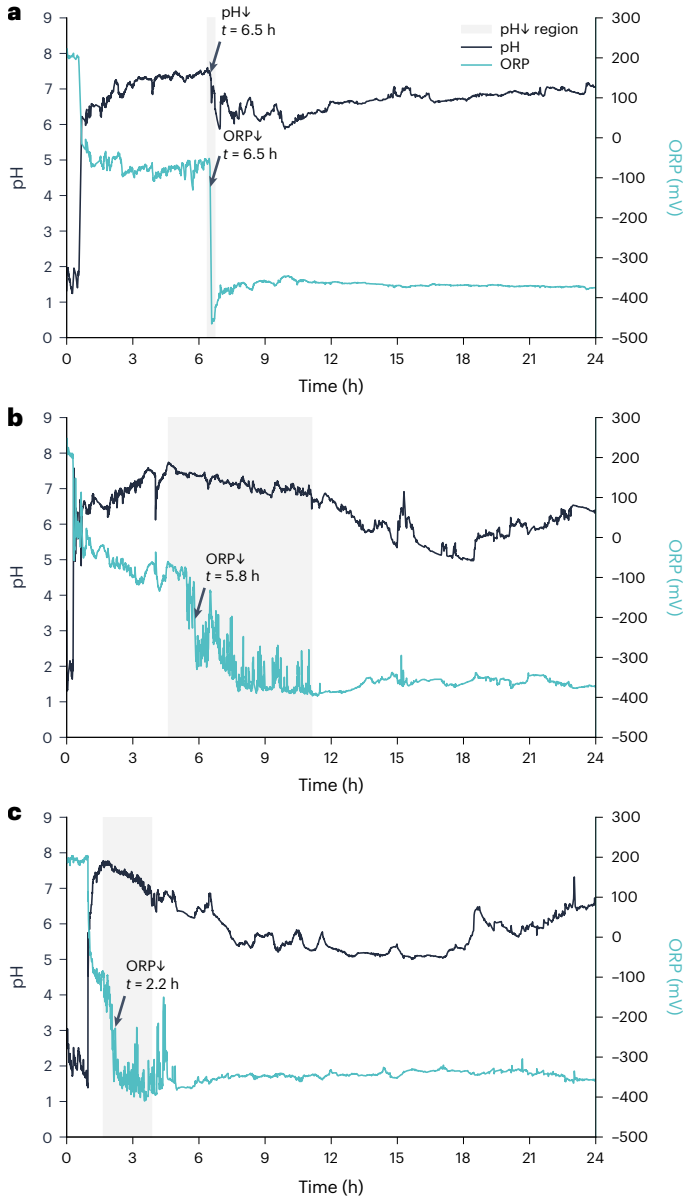

Fig. 6 | ORP measurements to support localization. a, Clear small intestine–large intestine transitions are visible in both pH and ORP, indicated by the two arrows. **b**, Example of a case in which it is difficult to pinpoint entry into the large intestine based on pH alone and ORP could be of added value. **c**, Another example, showing a big jump in ORP and only a gradual drop in pH. The grey shaded area shows the uncertainty region for pH. The ORP drop, indicated by the arrow, could help in these cases. For clarity of exposition, only the first 24 h of data are shown. *t*, time.

dropping[41]. This suggests that ORP measurements could be a better indication of the anatomical location of large-intestine entry. The combined ORP and pH measurements, transmitted to the receiver in real time every 20 s, offer superior localization compared to pH data alone.

Clinical impact and applications

The GISMO capsule offers easy, affordable and non-intrusive measurements of GI redox balance without requiring any unpleasant bowel preparation, providing a potential substantial clinical impact. Redox sensing gives a combined measure of various physiological processes essential for maintaining gut health and, consequently, overall well-being. Redox balance is not a specific measure of one process but rather a measure of a complex interplay between the host, gut microbiome and immune system that could be used to monitor a variety of gut disturbances.

In diseases and disorders of the GI tract, such as IBD and GI cancers, inflammation and dysregulation of the immune response combined with changes in the microbial community lead to an imbalance of oxidants and antioxidants[5,7,42]. For example, indirect markers of redox state in mucosal biopsies of IBD patients have shown a 10-fold to 100-fold increase in reactive oxygen metabolites[43,44]. Lacking tools to measure ORP in vivo, the direct impact of inflammation on redox potential can only be estimated from limited cell culture experiments. Research in neutrophils has shown that an induced inflammatory event leads to a significant, dose-dependent rise in ORP, providing a proof of concept for the use of an ingestible ORP sensor to detect inflammation[25]. An ingestible device that measures inflammation-related markers in the GI tract could significantly impact the patient journey, particularly in screening, stratification and monitoring. For instance, in IBD patients, about one-third do not respond to initial treatments, and half of the patients experience diminishing treatment effectiveness over time[45]. Inadequate treatment directly affects quality of life, and prolonged inflammation increases the risk of irreversible long-term damage to the intestinal wall[46]. There is a clear need for objective biomarkers that can help guide decisions on changing treatment, adjusting dosage or transitioning to surgery, to ensure that patients receive the right treatment as quickly as possible[47]. In follow-up trials with the GISMO ingestible, the potential of an ingestible ORP sensor to quantify both the severity of inflammation and its approximate location will be evaluated. These capabilities would enable more frequent monitoring compared to invasive procedures like colonoscopy or endoscopy and offer a more objective and timely assessment compared to symptom-based evaluations.

Redox balance in the gut plays a vital regulatory role not only in GI diseases but also in shaping overall health through its influence on the gut microbiome. Redox balance regulates how effectively bacteria can grow in a certain environment[3]. Our bodies' immune system uses this mechanism by modulating the chemical environment to fight off invaders[2]. Changes in redox potential affect not only pathogenic bacteria but also the large community of commensal gut microbes, which are a crucial element of the gut barrier[48,49]. The presented data show that in healthy people with an anticipated healthy microbiome, the large intestine is strongly reducing. Microbiome disturbances are expected to shift this balance to an unfavourable, more oxidative environment. Limited faecal and post mortem analyses in mice have shown that microbiome-disrupting antibiotics can induce ORP increases as large as 200–400 mV (refs. 49,50), far exceeding the 72-mV-wide range (5th–95th percentile) that we observed in the large intestine of our healthy population (see also the inter- and intra-participant variability displayed in Extended Data Fig. 4b).

The GISMO capsule has the potential to offer insights into microbiome function, moving beyond current methodologies that mainly rely on faecal samples. In cases of suspected dysbiosis, ingestible redox measurements could offer a comprehensive view of gut health across the entire GI tract. ORP measurements may also be easier to interpret compared to microbiome composition data, which can be challenging to analyse due to functional redundancy and high dimensionality. Further clinical studies are needed to provide deeper insights into how ORP changes are influenced by microbiome alterations: for example, involving individuals undergoing antibiotic treatment, given the drastic impact of antibiotics on the gut environment. Insights into this antibiotics-eradicated microbiome on the one hand and the microbiome of healthy people on the other hand could show the two extremes of the spectrum and create a foundation for the interpretation of gut redox studies in other contexts, such as the gut–brain axis, aging and (nutritional) interventions. In our small cohort of healthy volunteers, the data suggest that redox signals in the large intestine are relatively comparable between participants and remain stable over time, when comparing the five ingestibles administered per participant over a

four-month period. The redox signal was not significantly affected by our dietary intervention (Extended Data Fig. 7), although the diets were not specifically designed for that purpose. The diets were designed to create a contrast in protein fermentation. Besides the effect of dietary pro-oxidants and antioxidants that may survive absorption in the small intestine (for example, phenolic compounds), metabolites produced by microbiota during fermentation, of proteins but also carbohydrates, have a large effect on the intestinal environment and gut health[51,52]. The interplay between nutrition, microbiome and redox balance impacts fermentation and consequently the production of metabolites. We foresee that if these relationships are better understood in the future, the GISMO ingestible could play a role in personalized nutrition. Individuals with disrupted gut health could compare their data to (personal) reference values and assess how dietary and lifestyle changes might shift their data closer to their own previous healthy baseline or to a healthy reference population.

The in-human redox values reported in this study vary substantially along the GI tract. This is to be expected because there is a strong gradient of decreasing oxygen concentration and increasing microbial activity along the gut[39], both influencing redox potential. We observed that this variation of ORP along the tract could enhance localization of ingestibles. Incorporating ORP data alongside pH information could boost confidence in assessing regional transit times (for example, in studying motility disorders), guiding sampling and drug-release capsules and linking measurements to specific regions of the gut. Follow-up studies with a reference standard (such as ultrasound) should validate the use of ORP for localization. This variation along the tract also means that assessment of redox-based gut-health measures should be done per segment, based on group averages or, preferably, personalized predictions. In this work, we provide a reference dataset of gut redox values of healthy volunteers for the different GI segments.

A limitation of using ingestibles to assess gut health is the non-specificity of redox measurements. Although this can be an advantage as a general indicator of gut health, it may require supplementation with other clinical evaluations to achieve a specific diagnosis or provide tailored advice. Despite this limitation, given the scarcity of tools capable of directly objectively measuring inside the GI tract, even non-specific measurements can offer significant value. Follow-up studies are expected to provide greater insight into specific clinical applications. Another limitation of the GISMO ingestible is its inability to measure at a specific location, as it relies on gut motility. Additionally, long-term measurements with the same device are not feasible; wearable sensors are more suitable for that purpose. However, the ease of swallowing and minimal impact on the user make repeated measurements with the GISMO ingestible practical. A final limitation is the risk of device retention, especially in patients with strictures: for example, in patients with Crohn's disease. The small size of our capsule (three times smaller than camera capsules and a commonly used pH capsule) should reduce this risk, but those patients should be closely monitored.

Conclusions

We have reported the development, validation and clinical testing of ingestible sensors that can measure in vivo redox balance along the human gut. The sensors are designed to work without any unpleasant bowel preparation and provide real-life measurements. Further clinical investigations will be required to evaluate our GISMO ingestible sensor in patient populations. We anticipate that in vivo ORP measurements can offer functional insights into the gut microbiome and could enable easy localization and objective quantification of inflammation, facilitating improved disease diagnosis and monitoring. Given the central role of the gut in maintaining overall health, our ingestible sensors could enhance understanding of gut-linked diseases, the gut–brain axis, aging[53], (nutritional) interventions[5,6,54,55] and drug–gut interactions[5,56,57].

Methods

Ingestible architecture, sensors, electronic design and electrical testing

The ingestible architecture is shown in Fig. 2b. At the centre of that architecture is a low-power ARM Cortex M4F-based microcontroller (STM32L432, ST Microelectronics). It is used to control the system (sensing, communication, turn-on/off and so on) and to encrypt the data using AES-128. The system electronics were implemented on a stack of two 400-µm thin, four-layer high-density interconnect 5.8 mm × 10.8 mm PCBs, as shown in Fig. 2c. A third layer implements the sensor functionality on a 150-µm thin two-layer polyimide flexible PCB. This combination of thin rigid and flexible boards allowed optimizing the volume taken up by the electronics in a tradeoff between interconnect density and fine-pitch component assembly on the one hand and substrate thickness on the other hand. A simplified schematic diagram of the ingestible system electronics is shown in Supplementary Fig. 1. A sub-gigahertz radio transceiver from ST Microelectronics (S2LP) is used to communicate with the receiver, to receive device configuration and send measurement data.

We selected the conformal stepped impedance antenna design of ref. 30 as the basis for the GISMO pill antenna. Reference 30 showed that this type of conformal microstrip antenna radiates efficiently in lossy tissue, is robust against changes in dielectric loading caused by the surrounding tissue, occupies minimal volume in the pill (hence allowing maximum space for electronic circuitry and sensors) and aims for a communication range up to 15 m for deep (>5 cm depth) implants[58]. We optimized this conformal stepped impedance antenna for operation in the selected 868-MHz frequency band considering the dimensions, the dielectric properties of the filling material and the encapsulation selected for the GISMO pill. By adjusting the dimensions of the ground plane, the patch, the slots on the ground plane and the insets on the patch, we realized an efficient conformal antenna for the GISMO pill. The antenna is manufactured as a flexible circuit board etched out of copper on a polyimide substrate and measures 10 mm × 17 mm with a thickness of 172 µm. The antenna is attached to the inner wall of the PEEK tube that contains the electronics and is filled with epoxy. The simulated radiation efficiency (η) in a spherical phantom with a radius of 5 cm and filled with muscle tissue equalled 0.5%. This outperforms commercial small in-body antennas below 1 GHz, which show radiation efficiencies ranging between 0.02% and 0.3% (ref. 59). Immersed in a large body phantom of 40-cm diameter filled with muscle tissue, the optimized conformal stepped impedance antenna achieved a realized gain between −33.2 and −20.8 dBi (Extended Data Fig. 2). The negative value for the realized gain is a consequence of the lossy nature of human body tissue.

The entire communication was extensively validated in vitro in a large barrel (120 l, 40-cm diameter) filled with stomach-simulating liquid as described by ref. 60 (measured relative permittivity of 65.2 and conductivity of 1.17 S m^{-1} at 868 MHz). The −10-dB impedance bandwidth covered the targeted communication band at 868 MHz (ref. 39). Radio communication was verified at various distances between capsule and receiver. A reception rate of 95–100% was obtained at up to 20 cm (the centre of the 40-cm phantom, in line with the 95th-percentile waist circumference, females and males combined, as reported in the US National Health and Nutrition Examination Survey[61]). We found that at the chosen frequency, for the S2LP radio coupled to our custom antenna, +6 dBm (4 mW) of transmission power was sufficient for reliable communication.

For the ORP sensor, we used a platinum electrode on a Si/SiOx substrate (sputtering 40 nm Pt + 5 nm Cr as adhesion layer, 700 µm × 850 µm; MicruX). As shown in Supplementary Fig. 1, the ORP sensor voltage is measured with a high-impedance amplifier circuit (AD8505ACBZ, Analog Devices) with input current <1 pA and digitized by the microcontroller analog-to-digital converter. For the ISFETs, a readout circuit similar to the circuit described by ref. 62 was implemented. This circuit biases the

ISFET with a fixed current and source-drain voltage, essentially putting the ISFET in a source-follower configuration such that any threshold voltage shift due to pH change is transferred to the source node, where it is digitized by the microcontroller analog-to-digital converter. Finally, a temperature sensor is included (TMP117, Texas Instruments; resolution 0.0078 °C, accuracy ±0.1 °C), which is primarily used to confirm body exit. A 3D magnetometer (MMC5633, MEMSIC) and 3D accelerometer (MC3672, MEMSIC) are also included.

The RE was optimized to balance electrode impedance and drift. Three frit diameter sizes (0.8, 1.0 and 1.5 mm) were monitored for their drift behaviour in 0.1 M KCl (expected concentration of K^+ and Cl^- in our final application). After only 60 h, the RE with a 1.5 mm frit diameter resulted in a not acceptable drift (Extended Data Fig. 1). By reducing the diameter to 1 mm or even 0.8 mm, we obtained good performance: that is, a drift of 0.03 mV h^{-1}. Note that the RE was conditioned for 1 h in 3.3 M KCl before the investigation, which is a common practice with most commercial REs. Because the smallest frit diameter of 0.8 mm resulted in a larger impedance, we opted for the 1-mm frit diameter, which ensured the best compromise between drift and electrode impedance (Extended Data Fig. 1c,d). With the optimized frit of 1 mm, we monitored in total ten custom ingestible REs in 0.1 M KCl at 37 °C for two weeks using four commercial Ag/AgCl REs (Metrohm): custom ingestible REs 1–3 versus Metrohm RE 1, custom ingestible REs 4 and 5 versus Metrohm RE 2, custom ingestible REs 5 and 6 versus Metrohm RE 3, and custom REs 7–10 versus Metrohm RE 4 (Extended Data Fig. 1e). The resulting average drift was 0.042 ± 0.012 mV h^{-1}.

The capsule housing is manufactured from biocompatible PEEK by a milling process, with a window opening for the sensors. Assembly of the electronics, batteries, antenna and sensors into the housing is done in a manual process guided by tooling. To provide a hermetic seal, epoxy was used to seal off the sensor window. The epoxy was manually deposited by trained operators and freshly mixed to ensure a good seal, avoiding any ingress while at the same time avoiding undesired coverage of the sensors. Additionally, the complete capsule was filled with epoxy such that only the ORP, pH sensors and RE were exposed to the GI tract.

Wearable and benchtop receiver

The capsule communicates with a battery-powered wearable receiver (87 mm × 62 mm × 22 mm), which has the same S2LP (ST Microelectronics) radio as the ingestible. Sensor data are stored on non-volatile memory (microSD card, connector size 14 mm × 15.2 mm × 1.98 mm) and can be read out via USB. This receiver consists of a single custom PCB, a membrane keypad with two buttons and two bicolour LEDs, a circularly polarized patch antenna to match the capsule antenna characteristics and primary LR6 batteries. The electronics are packaged in a custom-designed milled polyoxymethylene enclosure. A schematic representation of the system is shown in Supplementary Fig. 2a.

In addition, a more versatile benchtop receiver (160 mm × 160 mm × 215 mm) with a commercially available omnidirectional antenna (OmniLOG 90200) was developed. This receiver consists of stacked development boards for the microcontroller and the radio and a custom PCB that implements non-volatile storage and a real-time clock battery. This wall-outlet-powered benchtop receiver can be connected to a laptop for live monitoring if needed. At night, it is placed beside the bed for additional data coverage. A schematic representation of the system is shown in Supplementary Fig. 2b.

In vitro sensor validation

For the in vitro validation in standard solutions, we used two types of commercially available ORP standards for the positive ORP values: (S1) 220 mV, pH 7 (Mettler Toledo), 180–220 mV at 37 °C; and (S2) 600-mV Redox standard (Supelco 80138, Sigma Aldrich). We chose the ORP standard 600 mV to verify the design of the electronics (upper design limit of 280 mV because higher values are not expected in the GI tract) and at the same time provide pH ~0 as part of pH sensor validation. We additionally prepared ORP standards outside the range of commercially available solutions by saturating pH buffers—pH 4 (S3) and pH 7 (S4)—with 0.2 g per 100 ml quinhydrone (CAS 106-34-3, 182960, Sigma Aldrich). The expected ORP values for the pH 7 buffer/quinhydrone (S4) were between 60 and 120 mV and for the pH 4 buffer/quinhydrone mixture (S3) between 230 and 290 mV (ref. 63). To prepare negative (reducing) ORP standards, we followed the ORP standard solution preparation based on phosphate buffers saturated with quinhydrone by dissolving 10 g of quinhydrone in 1 l phosphate buffer pH 7 stock solution, which has positive ORP values around 80 mV (S5)[25]. The negative ORP standard solution was reached by increasing the pH until we reached pH 14 by controlled addition of 0.1 M NaOH to 200 ml of ORP stock solution. We attempted to prepare four different negative ORP standards: −50 mV (S6), −300 mV (S7), −550 mV (S8) and −400 mV (S9). However, we noticed that both pH and ORP values changed over time during the measurements, and it was very challenging to achieve stable negative (reducing) ORP values. As a general note, quinhydrone solutions are stable only for a short time period, and measurements should be completed within 2 h.

The porcine GI fluids used for validation of the pH and ORP sensors were frozen immediately after collection and thawed a day before the experiment. The full sample collection protocol is described in our previous work[64]. Six types of digesta were available: stomach, small intestine, caecum, proximal colon, middle colon and rectum. Each type of digesta was divided into three beakers: beaker 1 for the three ingestibles, beaker 2 for the commercial pH sensor and beaker 3 for the commercial ORP sensor. The anaerobic chamber was set at 37 °C during the entire experiment. Gas concentrations were adjusted throughout the experiment to mimic the different GI segments of the stomach (atmospheric conditions), small intestine (10% O_2, 1.5% H_2 and 5% CO_2) and large intestine (1% O_2, 3% H_2 and 13% CO_2)[65].

Validation of our sensors in an animal model

In December 2022, seven healthy pigs (bodyweight 23.4 ± 2.1 kg) were selected for in vivo validation of our ingestible sensor. The experimental protocol was approved by the Animal Welfare Officer of Wageningen University and Research. The experiment was carried out at the Research Facility CARUS at Wageningen University & Research. Pigs were fed ad libitum with a complete pelleted diet. Pigs also had unlimited access to water. Pigs were housed on straw bedding with two or three pigs per pen (2.75 m × 1.38 m) and could freely move within the pen. To ensure good coverage, a total of 18 non-wearable receivers were placed along the perimeter of the pens.

Clinical study design and study execution

Clinical evaluation of the ingestibles was performed as part of the PROFUN study. The PROFUN study was a two-week dietary intervention study with a randomized crossover design. The experimental protocol was approved by the medical ethical committee of the East region of The Netherlands (NL84483.091.23) and registered at ClinicalTrials.gov (identifier NCT06161155). The main objectives of the PROFUN study were 2-fold: to test the feasibility of the GISMO system and to measure the effect of protein-source digestibility on ammonium production. The study was conducted from November 2023 until February 2024. Informed consent was obtained from all participants.

Individuals were recruited via a volunteer database of the Human Research Unit of Wageningen University & Research. Inclusion criteria were age 16 years and older, BMI 18.5–30 kg m^{-2}, regular bowel movements (at least one defecation per 48 h) and suitable veins for cannula insertion. Exclusion criteria included, among others, (history of) GI diseases, history of major abdominal surgery, swallowing disorders, dysphagia to food or pills, implanted electromedical devices and using medication that can alter GI motor function. See Supplementary Table 1 for an extensive list. Fifteen participants, eight women and seven men,

were included. These participants, age 52 ± 19 years (mean ± s.d.), were 176 ± 9 cm tall, with a body weight of 76.5 ± 13.3 kg and BMI of 24.6 ± 3.1 kg m^{-2}. Two male participants dropped out during the study due to availability and sickness unrelated to the PROFUN study or the ingestible device (Supplementary Fig. 4). For one participant (P03), who completed only phase 1 of the experiment (see below), this meant that insufficient data were available for this participant to be included in two of our analyses (and their associated figures and statistics). The statistical comparison of morning versus evening ingestibles utilized only measurements from phase 2, for which we had no data from P03. The analysis of within-participant consistency of the pH/ORP drop latencies in the small intestine required repeated measurements of this variable for each participant, but only one data point was available for P03. All other analyses, figures and summary statistics did include the available data from P03.

The study was divided into two phases. During phase 1, the feasibility of the GISMO system for safely monitoring biomarkers in the GI tract was assessed and baseline measurements were performed. Phase 2 was a randomized crossover controlled feeding trial to study the effect of protein digestibility on protein fermentation. During phase 2, participants adhered twice to a one-week fully controlled diet with a one-week washout period in between. During phase 1, participants swallowed one GISMO ingestible, and during phase 2, participants swallowed two ingestibles per dietary intervention (2 × 2); thus a total of five ingestibles were swallowed per participant (Supplementary Fig. 3). During the dietary intervention, participants were provided for 2 × 7 days with a diet supplemented with 30 g of protein per day (divided over three meals) either from bovine plasma protein, as a low-digestible protein, or whey protein isolate, as a high-digestible protein source. The proteins, lipids, carbohydrates and fibre contents were the same for both diets and corresponded to 12%, 36%, 50% and 2% (w/w) of total energy intake. Adherence to the dietary protocol was high, as assessed using self-reported food diaries. Forty percent of participants fully adhered to the prescribed diet, and all participants demonstrated more than 97% adherence. The diet intervention was designed for other research questions and appeared not of further relevance for the redox measurements. See also Extended Data Fig. 7 for a comparison of pH and ORP between the two diets.

Participants swallowed one GISMO ingestible after an overnight fast (12 h) during phase 1 and during both dietary interventions of phase 2. Except for the overnight fast, we did not request any additional preparation from the participants. In particular, no bowel preparation or cleansing of any sort was required. The ingestible was swallowed together with 200 ml lukewarm water. After swallowing the ingestible, participants drank approximately 150 ml of room temperature water every 15 min to study change in monitored temperature, which indicated whether the ingestible was still in the stomach or had moved to the small intestine. If the ingestible had passed into the small intestine, the relative cold water would not induce a drop in the monitored temperature. When the ingestible had left the stomach, or at most after 1 h of swallowing the ingestible, the participant was given a standardized breakfast meal. During phase 2, participants swallowed a second GISMO ingestible directly before their evening meal, also with 200 ml lukewarm water. Participants were given their evening meal directly after, regardless of whether the ingestible had left the stomach.

Safety and acceptance of the technology

The GISMO ingestible sensor system was designed and evaluated in accordance with the European Medical Device Regulation. Preclinical evaluation included, among others, biocompatibility testing, electrical safety assessment and electromagnetic compatibility (EMC).

Evaluation of biocompatibility in accordance with the ISO 10993-1:2018 standard was performed on the device and showed acceptable risk levels of sensitization, irritation, acute systemic toxicity and cytotoxicity endpoints.

EMC testing of the ingestible and receiver was evaluated in accordance with the IEC 60601-1-2:2014 standard, showing that both devices comply with EMC criteria for basic safety and the risk of data loss is acceptable. Also, an electrical safety risk analysis, related to IEC 60601-1:2005 requirements for electrical hazards, concluded that no unacceptable risks related to electrical hazards were present.

The long-term comfort of the wearable receiver was initially evaluated in a usability trial. The mechanical design, the clarity of the user interface and system stability under trial conditions of the wearable receiver were validated by a four-day trial involving six participants.

The PROFUN clinical trial participants were positive about the comfort of the ingestible and receiver. Participants were asked to score specific characteristics of the ingestible capsule from 1 (totally disagree) to 5 (totally agree). Results showed that participants found swallowing the ingestible very easy (4.5/5), they were more than willing to swallow multiple sensor capsules again (4.6/5), and they did not feel bothered by the idea of having an experimental sensor capsule inside their body (3.7/5) or restricted in their activities by the sensor capsule (3.7/5). Participants also did not feel restricted by wearing the wearable receiver on their body (3.2/5).

Also, no adverse events related to the device occurred during the entirety of the study. All ingestibles were excreted within eight days. We observed longer than expected transit times in some participants, potentially due to the dietary intervention. See Extended Data Table 1.

Sensor preparation, verification, calibration and acceptance range

The same sensor preparation steps were used for in vitro validation, in vivo validation and clinical trial. Ingestibles were disinfected before use (isopropyl alcohol 70%). The verification and calibration steps were all performed in a water bath at body temperature (37 °C).

The ORP sensors were verified using a one-point standard solution (51350060, 220 mV/pH 7, Mettler Toledo; 180–220 mV at 37 °C). Ideally, we would have conducted an additional verification for negative ORP values; however, due to lack of commercial standards in that range and the widely accepted practice of one-point verification—because redox electrodes typically maintain a stable zero point and slope over time—we chose the one-point verification.

The pH ISFETs were calibrated in four different pH standards of pH 2, 4, 7 and 9 (Avantor 20 °C AVS TITRINORM; accuracy ±0.02 pH units). An additional pH verification was performed with a PBS solution at pH 7.4. Calibration data were analysed to guarantee acceptable slope and offset (−49 mV per decade < slope < −56 mV per decade and 300 mV < offset < 1,300 mV) and used to convert the mV readings into pH values.

Clinical trial data processing

For each ingested pill, data were collected from two receiving devices: the wearable receiver and a non-wearable receiver for nighttime use; and in two cases, data were recovered from the flash memory of the ingestible. Flash memory is by design one-ninth of the data and is only meant to be a backup option; pills need to be recovered to read out the flash memory. These were merged into one dataset. Data deemed faulty or untrustworthy were excluded from further analysis, based on the following criteria. For one ingestible, one of the two pH sensors failed the prestudy calibration acceptance criteria, and thus data from this one pH sensor were not analysed. Out of 69 ingestibles, three ingestibles were completely removed from analysis, leaving 66 remaining for evaluation. One participant (P13) became ill and experienced GI symptoms during the second dietary intervention, and therefore data from this period (two ingestibles), which would not be representative of normal healthy gut conditions, were excluded. One ingestible had a premature shutdown due to battery failure in the stomach; this ingestible was removed because we did not have a complete GI segment. For another nine ingestibles—two other ingestibles with premature

shutdown due to battery failure, one in the small intestine and one in the large intestine, and seven ingestibles with unexpectedly long transit times that entered into ultra-low-power mode before excretion, resulting in incomplete coverage of some GI segments—only segments were analysed for which a beginning and end could be identified, and segment summary statistics were computed only if the ingestible had completed at least 80% of its transit time through a segment before pill shutdown. Finally, data points were excluded from analysis if they closely approached the range limits of the electronic circuit, which could occur in the case of a gas bubble temporarily covering a sensor or the RE. On average, 0.6% of measurements were excluded per ingestible, with a maximum of 12.2% (not including cases where entire ingestibles, sensors or segments were excluded). pH measurements were averaged across the two pH sensors before further analysis; when only one sensor was available, the measurement from that sensor was used. Two pH sensors showed an unrealistic large drift; for those ingestibles, only the other pH sensor was used. Data analysis was implemented in Python scripts using Python v.3.12 and Python packages numpy (v.1.26), scipy (v.1.14) and pandas (v.2.2).

Clinical trial sensor performance

To be able to confirm the performance of the sensors throughout the entire GI tract and their stability over time, we asked participants to collect all their faeces from the moment of ingestion until confirmed body exit. Retrieved ingestibles were washed and inspected with an optical microscope. We did not observe any sensor or capsule damage or deterioration. From the retrieved ingestibles from the clinical trial, we repeated the pH and ORP sensor validation post-ingestion in vitro in ORP (alternate) standard solutions using three ingestibles and two commercial ORP sensors. As shown in Extended Data Fig. 8, both pH and ORP sensors of the retrieved ingestibles from the clinical trial show performance similar to that of the new ingestibles (Fig. 3).

Clinical trial redox sensor performance

Pre-ingestion, all 66 analysed ORP sensors were within the expected 180–220 mV range, with an average of 204.6 ± 6.4 mV. For post-excretion verification, 63 sensors were available: one ingestible was flushed down the toilet, and two ingestibles were accidentally stored in the freezer by the participants—they were not designed for this and hence stopped working. With post-excretion values of 197.8 ± 9.8 mV, a neglectable absolute drift of 8.3 ± 6.2 mV was observed, and all but three sensors (176.8, 179.8, 227.3 mV) were within acceptance criteria.

Clinical trial pH sensor performance

During the calibration before ingestion, for all 66 analysed ingestibles, all but one of the 131 pH sensors were within the acceptance range, with an average slope of −54.0 ± 0.9 mV per decade and offset of 996.6 ± 102 mV. One pH sensor had a slightly lower slope (−47.9 mV per decade) than the acceptance criteria, and for that ingestible, the second pH sensor was used for further analysis.

We recalibrated the ingestibles after retrieval to assess sensor performance and drift. Of 63 available ingestibles, excluding one pH sensor that gave zero values, all pH sensors were within acceptance range with an average slope of −54.3 ± 0.7 mV per decade and offset of 982 ± 101.9 mV. The failed pH sensor during post-calibration was from a different ingestible than during pre-ingestion calibration, meaning that all 66 ingestibles had at least one working pH sensor throughout the GI tract.

Extended Data Fig. 9 shows example pH calibration profiles pre-ingestion and post-excretion for an ingestible with a median drift profile, the ingestible with the shortest transit time (14 h) and the ingestible with the longest transit (178 h). The sensitivity (slope) of all but one pH sensor remains similar between pre- and post- ingestion despite the harsh conditions in the GI tract and any potential fouling. The absolute sensor drift varied between 0 and 40.2 mV (after removing one extreme outlier with an unrealistic high drift of 75.2 mV; this sensor was excluded from all analyses (see 'Clinical trial data processing')) with an average 14.6 ± 10.6 mV. The offset drift did not appear to be linearly dependent on total transit time. For example, the absolute offset drifts of the ingestible with the shortest transit time (14 h) were 3.0 and 5.1 mV (0.20 and 0.36 mV h^{-1}), respectively, whereas the offset drifts of the ingestible with the longest transit time (178 h) were 12.9 and 17.6 mV (0.07 and 0.10 mV h^{-1}). All in all, we can conclude that both pH and ORP sensors showed good performance and stability over time throughout the entire GI tract.

Annotation of the sensor signals

The different segments of the GI tract were annotated based on pH recordings. Following guidelines from previous work[66], we relied on known pH fluctuations to segment our sensor time-series data into stomach, small-intestine and large-intestine compartments. Specifically, stomach exit was defined as the time of a sharp and sustained rise in pH (at least 2 units, not followed by any time points below a pH of 4.5). Transit from small intestine to large intestine (ileocecal junction) was defined as the beginning of a steep drop in pH of at least 0.5 units. Temperature readings were used to determine body exit. In addition, the timing of a sharp drop in ORP (at least 100 mV, with a starting value around −200 mV), shortly before the presumed entry into the large intestine, was also annotated.

Time-series alignment between ingestibles

To aggregate sensor time-series data across multiple ingestibles, which passed through participants' GI tracts at different (and varying) rates of travel, we aligned the signals from different ingestibles based on the GI compartment segmentations (see 'Annotation of the sensor signals'). Data from each segment were resampled from the original measurement times to a common time frame of 500 linearly spaced time points between segment start and end points, bringing data from different ingestibles into alignment and enabling summary statistics to be computed across corresponding data points. We refer to this method as 'linear rescaling'.

Statistical procedures

To determine whether sensor measurements differed reliably between different experimental conditions (for example, morning versus evening pills) at any moment in the capsules' transit through the GI tract, we employed a cluster-based permutation test[67]. Briefly, a cluster is defined as a set of contiguous time points that all individually exceed a statistical threshold of $P < 0.05$ (two-sided) based on a (paired) t-test. The magnitude of a cluster is defined as the cumulative t-statistic across its constituent time points. A null distribution of cluster magnitudes is then constructed by permuting the data N times, each time swapping the condition labels of a random subset of signals and recording the maximum cluster magnitude observed in each permuted data sample. Finally, a (two-sided) P value is assigned to each cluster observed in the original (not permuted) data by computing the proportion of cluster magnitudes recorded across data permutations that exceeded the observed cluster's magnitude: $P = \frac{k+1}{N+1}$, where k is the number of data permutations for which the (absolute) maximum cluster magnitude exceeded the (absolute) observed cluster magnitude.

Around the (apparent) time of entry into the large intestine, both the ORP and pH signals reliably exhibit a drop, but the relative timing of these events is variable. To determine whether this timing was consistent within participants, a Kruskal–Wallis test was performed on the latency of the pH drop compared to the ORP drop, with participant as the grouping variable, and a corresponding effect size was calculated as $\eta^2 = \frac{H-k+1}{n-k}$, where H is the Kruskal–Wallis test statistic, k is the number of groups and n is the total number of data points.

Reporting summary

Further information on research design is available in the Nature Portfolio Reporting Summary linked to this article.

Data availability

Access to underlying data, information on other study parameters and other types of subsets requires controlled access, given that the nature of the data falls under special categories of personal data. Hence, processing of these data is subjected to specific provisions and requirements as set out in General Data Protection Regulation 2017/679. Restrictions related to existing data-sharing agreements between concerned parties involved may apply. The data that support the findings of this study can be made available upon request to the corresponding author within the limitations of the applicable regulations and ethical limitations. We intend to respond to data requests within three months.

References

1. Lee, J. Y., Tsolis, R. M. & Bäumler, A. J. The microbiome and gut homeostasis. *Science* **377**, eabp9960 (2022).
2. Campbell, E. L. & Colgan, S. P. Control and dysregulation of redox signalling in the gastrointestinal tract. *Nat. Rev. Gastroenterol. Hepatol.* **16**, 106–120 (2019).
3. Husson, O. Redox potential (Eh) and pH as drivers of soil/plant/microorganism systems: a transdisciplinary overview pointing to integrative opportunities for agronomy. *Plant Soil* **362**, 389–417 (2013).
4. Sies, H. Oxidative stress: a concept in redox biology and medicine. *Redox Biol.* **4**, 180–183 (2015).
5. Bourgonje, A. R. et al. Oxidative stress and redox-modulating therapeutics in inflammatory bowel disease. *Trends Mol. Med.* **26**, 1034–1046 (2020).
6. Penumutchu, S., Korry, B. J., Hewlett, K. & Belenky, P. Fiber supplementation protects from antibiotic-induced gut microbiome dysbiosis by modulating gut redox potential. *Nat. Commun.* **14**, 5161 (2023).
7. Yangyanqiu, W., Jian, C., Yuqing, Y., Zhanbo, Q. & Shuwen, H. Gut microbes involvement in gastrointestinal cancers through redox regulation. *Gut Pathog.* **15**, 35 (2023).
8. Vaccaro, A. et al. Sleep loss can cause death through accumulation of reactive oxygen species in the gut. *Cell* **181**, 1307–1328.e15 (2020).
9. Baltsavias, S. et al. In vivo wireless sensors for gut microbiome redox monitoring. *IEEE Trans. Biomed. Eng.* **67**, 1821–1830 (2019).
10. Koopman, J. P., Janssen, F. G. J. & Van Druten, J. A. M. Oxidation-reduction potentials in the cecal contents of rats and mice (38942). *Proc. Soc. Exp. Biol. Med.* **149**, 995–999 (1975).
11. Geertsema, S. et al. Unsuitability of the oxidation-reduction potential measurement for the quantification of fecal redox status in inflammatory bowel disease. *Biomedicines* **11**, 3107 (2023).
12. Katerji, M., Filippova, M. & Duerksen-Hughes, P. Approaches and methods to measure oxidative stress in clinical samples: research applications in the cancer field. *Oxid. Med. Cell Longev.* **2019**, 1279250 (2019).
13. Azzi, A. Oxidative stress: what is it? Can it be measured? Where is it located? Can it be good or bad? Can it be prevented? Can it be cured? *Antioxidants* **11**, 1431 (2022).
14. Murphy, M. P. et al. Guidelines for measuring reactive oxygen species and oxidative damage in cells and in vivo. *Nat. Metab.* **4**, 651–662 (2022).
15. Cummins, G. et al. Gastrointestinal diagnosis using non-white light imaging capsule endoscopy. *Nat. Rev. Gastroenterol. Hepatol.* **16**, 429–447 (2019).
16. Li, Z., Liao, Z. & McAlindon, M. (eds) *Handbook of Capsule Endoscopy* (Springer, 2014); https://doi.org/10.1007/978-94-017-9229-5
17. Cao, Q. et al. Robotic wireless capsule endoscopy: recent advances and upcoming technologies. *Nat. Commun.* **15**, 4597 (2024).
18. Bacsur, P. et al. Effects of bowel cleansing on the composition of the gut microbiota in inflammatory bowel disease patients and healthy controls. *Therap. Adv. Gastroenterol.* **16**, (2023).
19. Timm, D. et al. The use of a wireless motility device (SmartPill) for the measurement of gastrointestinal transit time after a dietary fibre intervention. *Br. J. Nutr.* **105**, 1337–1342 (2011).
20. Soucasse, A. et al. Assessment of the smartpill, a wireless sensor, as a measurement tool for intra-abdominal pressure (IAP). *Sensors* **24**, 54 (2024).
21. Brunk, T. et al. Telemetric capsule-based upper gastrointestinal tract–blood detection–first multicentric experience. *Minim. Invasive Ther. Allied Technol.* **31**, 704–711 (2022).
22. Kalantar-Zadeh, K. et al. A human pilot trial of ingestible electronic capsules capable of sensing different gases in the gut. *Nat. Electron.* **1**, 79–87 (2018).
23. Dawson, M. A., Cheung, S. N., La Frano, M. R., Nagpal, R. & Berryman, C. E. Early time-restricted eating improves markers of cardiometabolic health but has no impact on intestinal nutrient absorption in healthy adults. *Cell Rep. Med.* **5**, 101363 (2024).
24. Inda-Webb, M. E. et al. Sub-1.4 cm^3 capsule for detecting labile inflammatory biomarkers in situ. *Nature* **620**, 386–392 (2023).
25. Gopalakrishnan, S. et al. Smart capsule for monitoring inflammation profile throughout the gastrointestinal tract. *Biosens. Bioelectron. X* **14**, 100380 (2023).
26. Mimee, M. et al. An ingestible bacterial-electronic system to monitor gastrointestinal health. *Science* **918**, 915–918 (2018).
27. You, S. S. et al. An ingestible device for gastric electrophysiology. *Nat. Electron.* **7**, 497–508 (2024).
28. Moglia, A., Menciassi, A., Dario, P. & Cuschieri, A. Capsule endoscopy: progress update and challenges ahead. *Nat. Rev. Gastroenterol. Hepatol.* **6**, 353–361 (2009).
29. Thwaites, P. A. et al. Comparison of gastrointestinal landmarks using the gas-sensing capsule and wireless motility capsule. *Aliment Pharm. Ther.* **56**, 1337–1348 (2022).
30. Nikolayev, D., Zhadobov, M., Le Coq, L., Karban, P. & Sauleau, R. Robust ultraminiature capsule antenna for ingestible and implantable applications. *IEEE Trans. Antennas Propag.* **65**, 6107–6119 (2017).
31. Abdigazy, A. et al. End-to-end design of ingestible electronics. *Nat. Electron.* **7**, 102–118 (2024).
32. Nandhra, G. K. et al. Normative values for region-specific colonic and gastrointestinal transit times in 111 healthy volunteers using the 3D-transit electromagnet tracking system: influence of age, gender, and body mass index. *Neurogastroenterol. Motil.* **32**, e13734 (2020).
33. Wang, Y. T. et al. Regional gastrointestinal transit and pH studied in 215 healthy volunteers using the wireless motility capsule: influence of age, gender, study country and testing protocol. *Aliment Pharm. Ther.* **42**, 761–772 (2015).
34. Mi, J., Peng, H., Wu, Y., Wang, Y. & Liao, X. Diversity and community of methanogens in the large intestine of finishing pigs. *BMC Microbiol.* **19**, 1–9 (2019).
35. Huang, Y., Marden, J. P., Julien, C. & Bayourthe, C. Redox potential: an intrinsic parameter of the rumen environment. *J. Anim. Physiol. Anim. Nutr.* **102**, 393–402 (2018).
36. Ziegler, A., Gonzalez, L. & Blikslager, A. Large animal models: the key to translational discovery in digestive disease research. *Cell. Mol. Gastroenterol. Hepatol.* **2**, 716–724 (2016).
37. Rowan, A. M., Moughan, P. J., Wilson, M. N., Maher, K. & Tasman-Jones, C. Comparison of the ileal and faecal digestibility of dietary amino acids in adult humans and evaluation of the pig as a model animal for digestion studies in man. *Br. J. Nutr.* **71**, 29–42 (1994).

38. *Dietary Protein Quality Evaluation in Human Nutrition* (FAO, 2013).
39. McCallum, G. & Tropini, C. The gut microbiota and its biogeography. *Nat. Rev. Microbiol.* **22**, 105–118 (2024).
40. Schneider, F. et al. Resolving the physiological conditions in bioavailability and bioequivalence studies: comparison of fasted and fed state. *Eur. J. Pharm. Biopharm.* **108**, 214–219 (2016).
41. Zarate, N. et al. Accurate localization of a fall in pH within the ileocecal region: validation using a dual-scintigraphic technique. *Am. J. Physiol. Gastrointest. Liver Physiol.* **299**, 1276–1286 (2010).
42. Winter, S. E. et al. Host-derived nitrate boosts growth of E. coli in the inflamed gut. *Science* **339**, 708–711 (2013).
43. Simmonds, N. J. et al. Chemiluminescence assay of mucosal reactive oxygen metabolites in inflammatory bowel disease. *Gastroenterology* **103**, 188–196 (1992).
44. Anezaki, K. et al. Correlations between Interleukin-8, and myeloperoxidase or luminol-dependent chemiluminescence in inflamed mucosa of ulcerative colitis. *Intern. Med.* **37**, 253–258 (1998).
45. Atreya, R. & Neurath, M. F. Biomarkers for personalizing IBD therapy: the quest continues. *Clin. Gastroenterol. Hepatol.* **22**, 1353–1364 (2024).
46. Ananthakrishnan, A. N., Kaplan, G. G. & Ng, S. C. Changing global epidemiology of inflammatory bowel diseases: sustaining health care delivery into the 21st century. *Clin. Gastroenterol. Hepatol.* **18**, 1252–1260 (2020).
47. Vieujean, S. et al. Understanding the therapeutic toolkit for inflammatory bowel disease. *Nat. Rev. Gastroenterol. Hepatol.* https://doi.org/10.1038/s41575-024-01035-7 (2025).
48. Homolak, J. Gastrointestinal redox homeostasis in ageing. *Biogerontology* **24**, 741–752 (2023).
49. Reese, A. T. et al. Antibiotic-induced changes in the microbiota disrupt redox dynamics in the gut. *elife* **7**, 1–22 (2018).
50. Meynell, G. G. Antibacterial mechanisms of the mouse gut II: the role of Eh and volatile fatty acids in the normal gut. *Br. J. Exp. Pathol.* **44**, 209–219 (1963).
51. Gilbert, M. S., Ijssennagger, N., Kies, A. K. & Van Mil, S. W. C. Protein fermentation in the gut; implications for intestinal dysfunction in humans, pigs, and poultry. *Am. J. Physiol. Gastrointest. Liver Physiol.* https://doi.org/10.1152/ajpgi.00319.2017 (2020).
52. Desai, M. S. et al. A dietary fiber-deprived gut microbiota degrades the colonic mucus barrier and enhances pathogen susceptibility. *Cell* **167**, 1339–1353.e21 (2016).
53. Finkel, T. & Holbrook, N. J. Oxidants, oxidative stress and the biology of ageing. *Nature* **408**, 239–247 (2000).
54. Kanarek, N., Petrova, B. & Sabatini, D. M. Dietary modifications for enhanced cancer therapy. *Nature* **579**, 507–517 (2020).
55. Zhang, G. et al. Artificial mucus layer formed in response to ROS for the oral treatment of inflammatory bowel disease. *Sci. Adv.* **10**, eado8222 (2024).
56. Jose, S., Bhalla, P. & Suraishkumar, G. K. Oxidative stress decreases the redox ratio and folate content in the gut microbe, Enterococcus durans (MTCC 3031). *Sci. Rep.* **8**, 12138 (2018).
57. Li, X. et al. Precise modulation and use of reactive oxygen species for immunotherapy. *Sci. Adv.* **10**, eadl0479 (2024).
58. Nikolayev, D., Zhadobov, M., Karban, P. & Sauleau, R. Conformal antennas for miniature in-body devices: the quest to improve radiation performance. *URSI Radio Sci. Bull.* **2017**, 52–64 (2017).
59. Nikolayev, D., Zhadobov, M., Sauleau, R. & Karban, P. in *Advances in Body-Centric Wireless Communication: Applications and State-of-the-Art* (eds Abbasi, Q. H. et al.) Ch. 6 (IET, 2016); https://doi.org/10.1049/PBTE065E_CH6
60. Van Nunen, T., Huismans, E., Mestrom, R., Bentum, M. & Visser, H. DIY electromagnetic phantoms for biomedical wireless power transfer experiments. In *Proc. IEEE Wireless Power Transfer Conference* 399–404 (IEEE, 2019); https://doi.org/10.1109/WPTC45513.2019.9055704
61. National health and nutrition examination survey 2017–2018. *CDC* https://wwwn.cdc.gov/nchs/nhanes/continuousnhanes/default.aspx?BeginYear=2017 (2018).
62. Chung, W.-Y. et al. in *Solid State Circuits Technologies* (ed. Swart, J. W.) Ch. 21 (IntechOpen, 2010); https://doi.org/10.5772/6891
63. *Alternate ORP Calibration Procedure* (Advanced Sensor Technologies, 2024); https://astisensor.com/wp-content/uploads/2024/09/Alternate_ORP_Calibration_Procedure.pdf
64. Leonardi, F. et al. Sensing the impact of diet composition on protein fermentation by direct electrochemical NH4+ sensing in gastrointestinal digesta. *Biosens. Bioelectron. X* **15**, 100406 (2023).
65. Zheng, L., Kelly, C. J. & Colgan, S. P. Physiologic hypoxia and oxygen homeostasis in the healthy intestine. A review in the theme: cellular responses to hypoxia. *Am. J. Physiol. Cell Physiol.* **309**, C350–C360 (2015).
66. Mikolajczyk, A. E., Watson, S., Surma, B. L. & Rubin, D. T. Assessment of tandem measurements of pH and total gut transit time in healthy volunteers. *Clin. Transl. Gastroenterol.* **6**, e100 (2015).
67. Maris, E. & Oostenveld, R. Nonparametric statistical testing of EEG- and MEG-data. *J. Neurosci. Methods* **164**, 177–190 (2007).

Acknowledgements

We acknowledge financial support by the province of Gelderland, the Netherlands. This work is also supported by the European Commission through the Horizon 2020 Programme, under GA AUTOCAPSULE (contract no. 952118). We thank J. Sombeek, G. van Amerongen and E. Erbas for their regulatory support; D. Young for the mechanical design of the wearable receiver and design support; J. Willem de Wit, J. van der Veer, M. Sadri, L. van Wyk, A. Beylik, J. de Leeuw, R. van Hardeveld, A. Patel and S. Fernandez Santos for their technical support; the staff at Carus Animal Research Facility for their assistance during the animal study; and all the volunteers who participated in the clinical trial.

Author contributions

A.E., T. Torfs, A.G., N.V.H. and C.V.H. were responsible for conceptualization of ingestible sensing. A.E., T. Torfs, F.L., A.v.H., R.S., D.F., I.D.C.M., R.R., G.V., K.M. and N.V.H. designed and validated the devices, sensors and infrastructure. R.M. and S.d.V. coordinated the animal study. A.E., R.M., E.C., R.A., S.d.V. and G.H. designed the clinical trial. R.M., F.L., A.v.H., R.S. and D.F. executed the clinical trial. A.E., R.M., T. Torfs, F.L., A.v.H., R.S., D.F., T. Teichmann, R.v.B. and K.M. carried out the data analysis, visualization and interpretation. A.E., R.M., T. Torfs, F.L., A.v.H., R.S., D.F., I.D.C.M., R.R., T. Teichmann, R.v.B., R.A., K.M. and N.V.H. wrote the paper. All authors reviewed and approved the paper.

Competing interests

A.E., F.L., N.V.H. and R.A. have filed a patent application on sensing in the GI tract with the European (EP4197437A1) and US (US20230190178A1) patent office. F.L., A.E. and R.S. have filed a patent application on measuring and localizing inflammation in the gut (application no. EP 24217111.4) with the European patent office. T. Torfs, I.D.C.M., A.E. and F.L. have filed a patent application on localization of an ingestible device (application no. EP24222150.5). The remaining authors declare no competing interests.

Additional information

Extended data is available for this paper at https://doi.org/10.1038/s41928-025-01411-4.

Supplementary information The online version contains supplementary material available at https://doi.org/10.1038/s41928-025-01411-4.

Correspondence and requests for materials should be addressed to Aniek Even.

Peer review information *Nature Electronics* thanks Alex Abramson, Yong Lin Kong and Khalil Ramadi for their contribution to the peer review of this work.

https://doi.org/10.1038/s41928-025-01411-4

Extended Data Table 1 | Regional and total transit times as measured by the GISMO ingestible

Parameter	Group	*N*	Median (h:min)	Min (h:min)	Max (h:min)	5th percentile (h:min)	95th percentile (h:min)
Gastric emptying time	All	66	01:11	00:03	13:12	00:18	11:12
	Baseline	15	00:39	00:18	01:16	00:20	01:13
	Diet WPI	24	04:31	00:03	13:12	00:33	12:06
	Diet BPP	27	04:29	00:06	11:13	00:13	10:58
	Morning	41	00:46	00:03	05:35	00:11	05:00
	Evening	25	09:48	01:08	13:12	01:49	12:04
Small intestinal transit time	All	65	06:17	01:33	10:38	03:00	09:05
	Baseline	15	06:15	02:21	09:39	03:27	09:16
	Diet WPI	24	06:13	01:33	10:04	02:49	08:35
	Diet BPP	26	06:52	02:48	10:38	03:53	08:55
	Morning	41	06:18	02:21	10:38	03:45	09:39
	Evening	24	06:07	01:33	08:45	02:50	08:24
Large intestinal transit time	All	65	45:58	06:07	168:48	13:54	121:37
	Baseline	15	41:00	13:34	97:32	16:18	90:39
	Diet WPI	24	45:13	13:03	138:37	16:26	114:07
	Diet BPP	26	54:42	06:07	168:48	08:31	140:47
	Morning	41	45:07	06:17	168:48	15:13	121:57
	Evening	24	51:17	06:07	147:04	13:58	117:47
Whole gut transit time	All	66	61:46	14:13	178:03	22:36	133:18
	Baseline	15	49:01	22:26	104:28	23:01	97:41
	Diet WPI	24	52:36	15:45	146:28	23:27	121:34
	Diet BPP	27	71:40	14:13	178:03	17:53	151:50
	Morning	41	51:51	15:34	178:03	23:04	132:55
	Evening	25	73:03	14:13	159:45	17:47	130:18

The ingestibles are grouped in the different experimental conditions. All: summarizing the data of the 66 ingestibles of the entire study; Baseline: data of phase 1 of the study, participants are on their habitual diet, ingestibles are given in the morning; Diet WPI: Whey Protein Isolate diet intervention, including the morning and evening pills; Diet BPP: Bovine Plasma Protein, including the morning and evening pills; Morning: all ingestibles given in the morning, including baseline WPI and BPP diet; Evening: all ingestibles given in the evening, including WPI and BPP diet. Note one of the ingestibles had a premature shutdown in the small intestine, hence missing small and large intestinal transit times, retrieval of the pill gave us the whole gut transit time.

https://doi.org/10.1038/s41928-025-01411-4

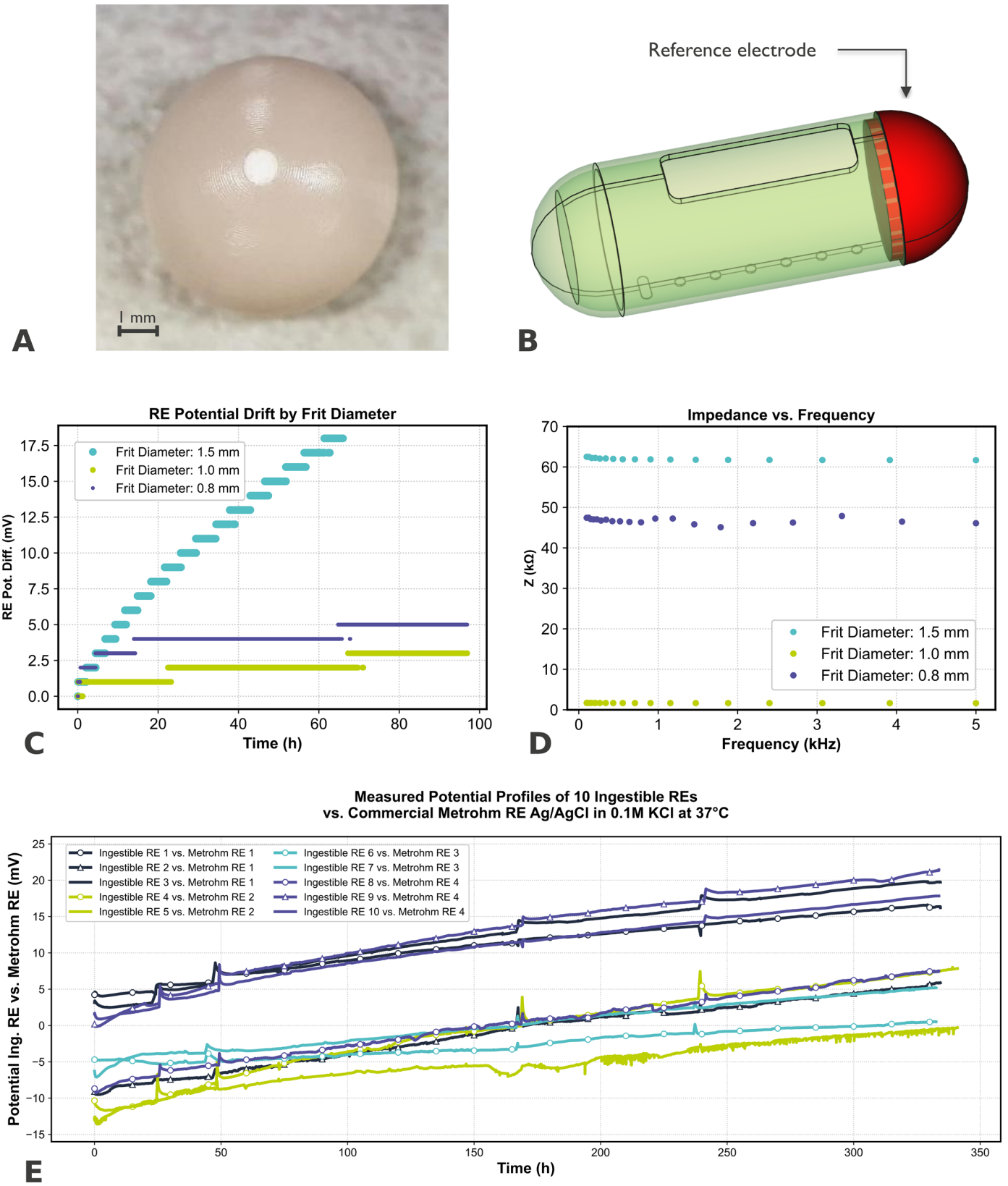

Extended Data Fig. 1 | Reference electrode (RE) design and optimization. (**a**) Optical image of the RE dome of the ingestible; the white circular area represents the porous frit material. (**b**) 3D drawing of the ingestible case where the red dome represents the reference electrode volume. (**c**) Drift and (**d**) electrochemical impedance study of a series of RE having three different frit diameters, that is 0.8, 1 and 1.5 mm. The diameter of the porous frit was evaluated to optimize the RE performance. The RE with a 1 mm frit diameter shows the best compromise in terms of drift and electrochemical impedance. (**e**) Potential profile of 10 ingestible reference electrode versus a commercial Ag/AgCl RE recorded in 0.1 M KCl at 37 °C. The potential of the REs was monitored for more than 325 h showing highly reproducibility and an overall drift < 0.06 V/h.

https://doi.org/10.1038/s41928-025-01411-4

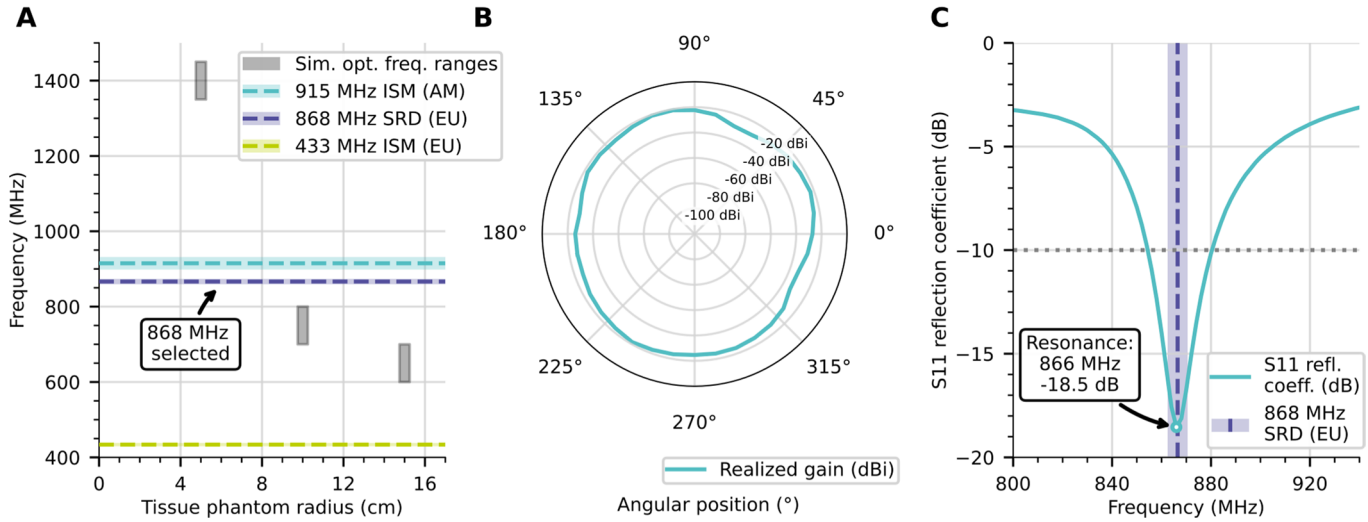

Extended Data Fig. 2 | Optimization and performance of the custom-designed ingestible antenna. (**a**) Overview of simulated optimal communication frequencies from an in-body capsule for different capsule depths. Simulation of an ingestible communicating from the center of spherical phantoms of different radius show the selected 868 MHz band as the most optimal license-free band that will work well over a various range of capsule depths. (**b**) Measured realized gain of the antenna in a large phantom of 40 cm diameter filled with muscle tissue, with values between −33.2 dBi and −20.8 dBi. Negative value is a consequence of the lossy nature of the human body tissue. (**c**) Measured S11 reflection of used antenna in phantom.

https://doi.org/10.1038/s41928-025-01411-4

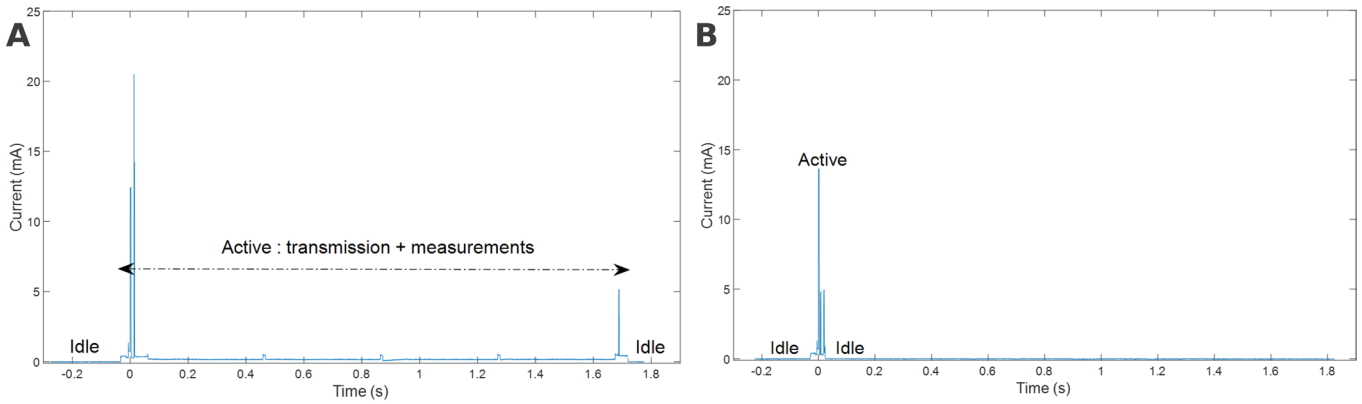

C

Ingestible	Started	Finished	Operation time in full functionality	Operation time in reduced functionality	Total operation time
S1	9/06/2023 15:24	12/07/2023 22:27	5 days	28.29 days	33.3 days
S2	22/06/2023 9:36	16/07/2023 8:15	5 days	18.94 days	23.95 days

Extended Data Fig. 3 | GISMO ingestible device power consumption. (**a**) Power profile in full functionality mode (all capsule sensor signals measured). (**b**) Power profile in reduced functionality mode (limited subset of signals measured, aiming to detect ingestible excretion or confirm its in-body presence for longer time than expected). (**c**) Operation time obtained from tests in the oven, confirming the 5 days in full functionality mode and well over the required 14 days including reduced functionality mode.

https://doi.org/10.1038/s41928-025-01411-4

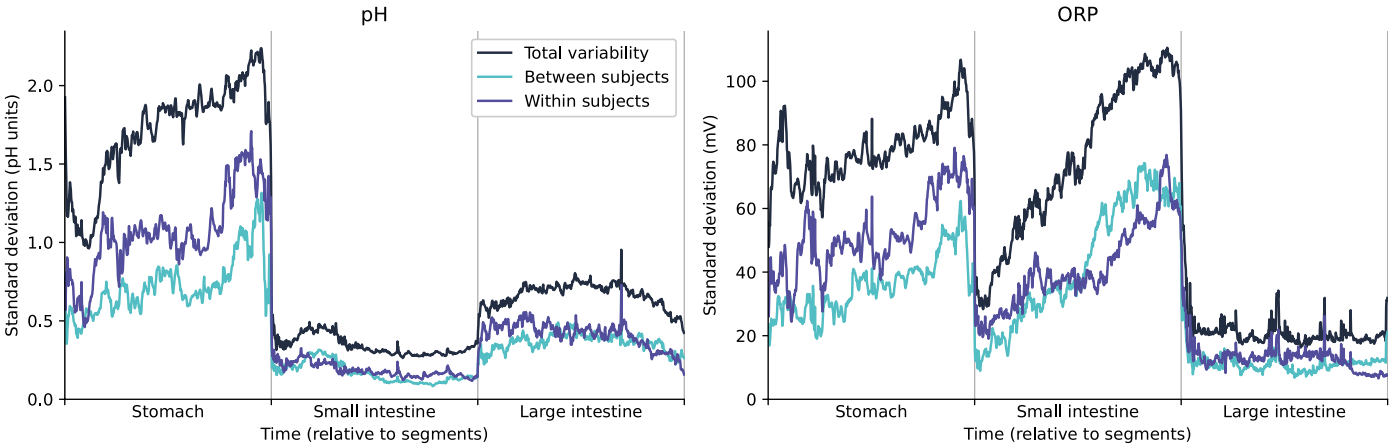

Extended Data Fig. 4 | Between- and within-subject variability in pH and ORP measurements. Variability was calculated over linearly rescaled pH (left panel) and ORP (right panel) time courses. This analysis only included subjects for whom data from all five experimental conditions were available. Total variability was calculated as the standard deviation across all ingestibles (for each rescaled time point – this is equivalent to the shaded error margins presented in Fig. 5a). To calculate between-subject variability, time courses were first averaged across all conditions (diets and morning and evening pills) for each subject, and then the standard deviation was computed across these subject-average time courses. Strict within-subject, repeated-measurements variability is somewhat challenging to estimate on our data, since no experimental condition was precisely repeated within the experiment. However, while we saw clear differences between morning and evening ingestibles (Fig. 5b), no significant differences could be detected between ingestibles swallowed the WPI and BPP diets (Extended Data Fig. 7). For the purposes of this analysis, we therefore take these as our best available proxy of repeated measurements (two measurements each, of the morning and evening conditions) and calculated the standard deviation across these data points. Note that there is high variability in the stomach for both sensor modalities, due the ingestion of food and drink, which can cause dramatic fluctuations in the chemical composition of the stomach contents. In the small intestine, a clear difference can be seen between pH and ORP, with the former being far more consistent. ORP is especially variable towards the end of the small intestine, as we noted previously, but appears to be more consistent within, than between subjects there. This is consistent with our observation that the relative timing of the ORP and pH drops towards the end of the SI was also somewhat consistent within subjects. Interestingly, ORP is very stable in the large intestine of these healthy subjects, which lends confidence that these measurements represent a reliable healthy baseline against which deviations, linked to disturbances in gut health, might be detected. Finally, it is worth bearing in mind that the variability shown in these plots can be caused by differences in sensor measurements at a given location in the gut, or by differences in the rates of transit of different capsules through different stages of the GI tract.

https://doi.org/10.1038/s41928-025-01411-4

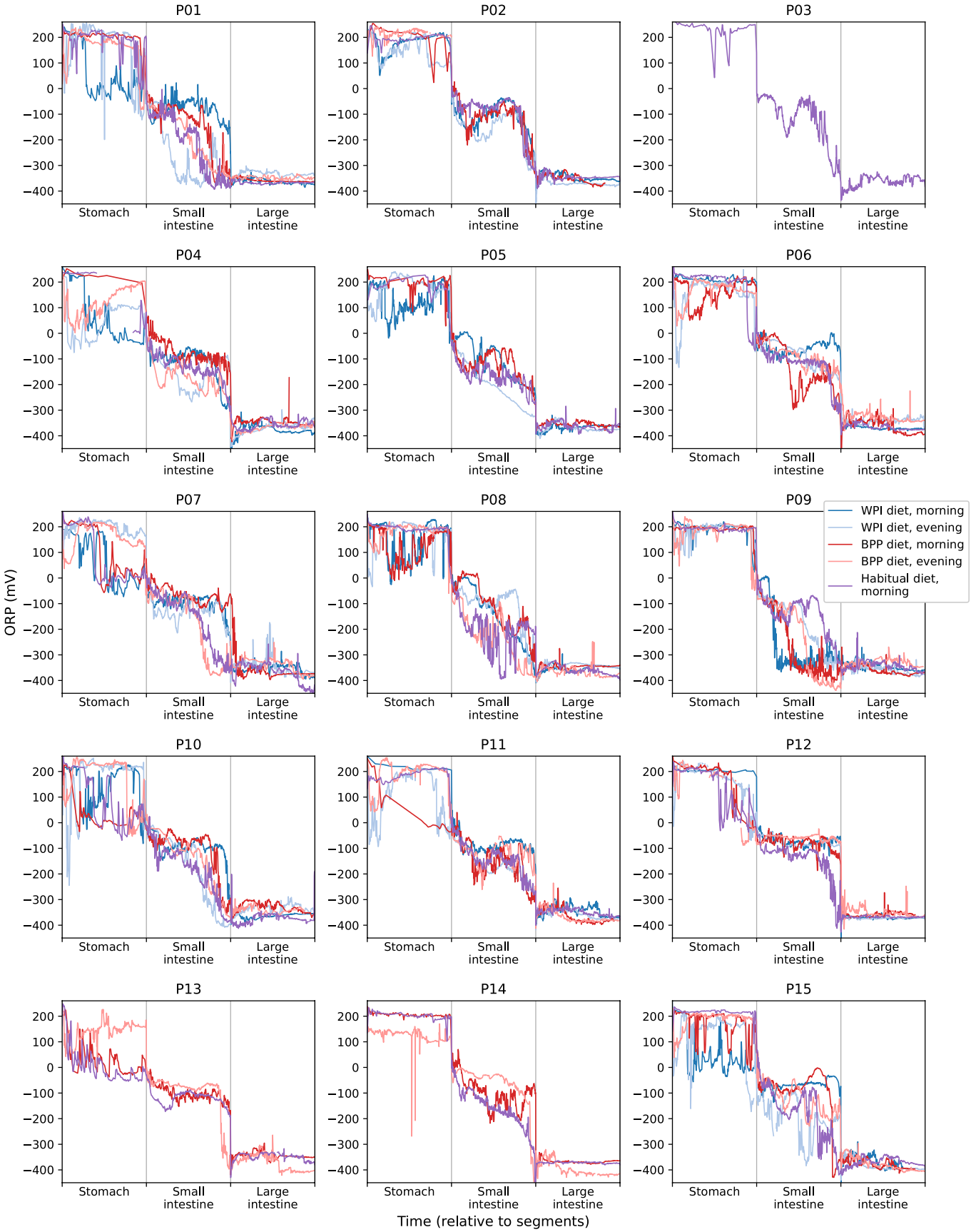

Extended Data Fig. 5 | Overview of all observed ORP profiles. ORP signals from all ingestibles, linearly rescaled to equal-duration segments (stomach, small intestine and large intestine), and plotted in separate panels for each of the 15 participants, with up to 5 different conditions for each participant plotted in different colors.

https://doi.org/10.1038/s41928-025-01411-4

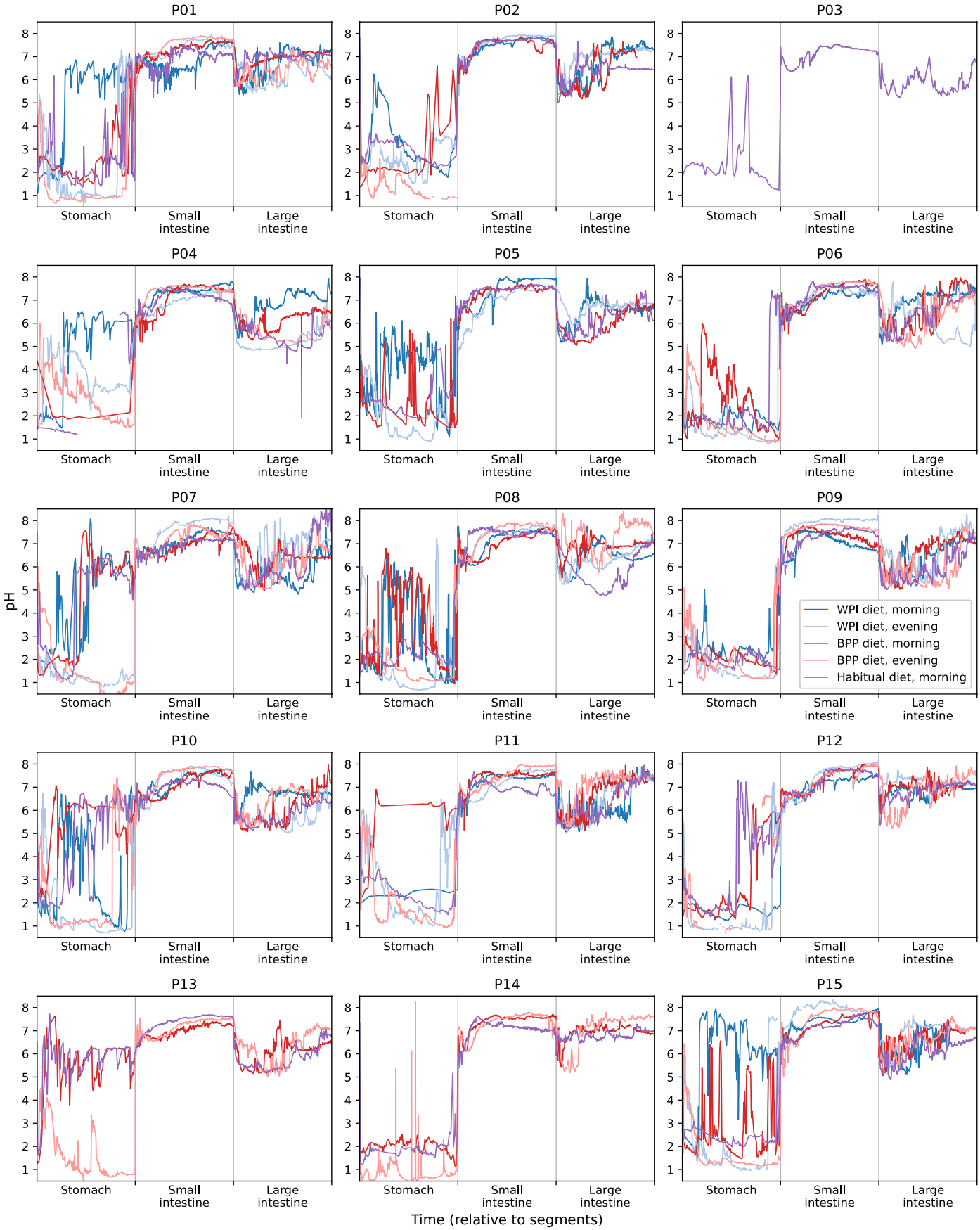

Extended Data Fig. 6 | Overview of all observed pH profiles. pH signals from all ingestibles, linearly rescaled to equal-duration segments (stomach, small intestine and large intestine), and plotted in separate panels for each of the 15 participants, with up to 5 different conditions for each participant plotted in different colors.

https://doi.org/10.1038/s41928-025-01411-4

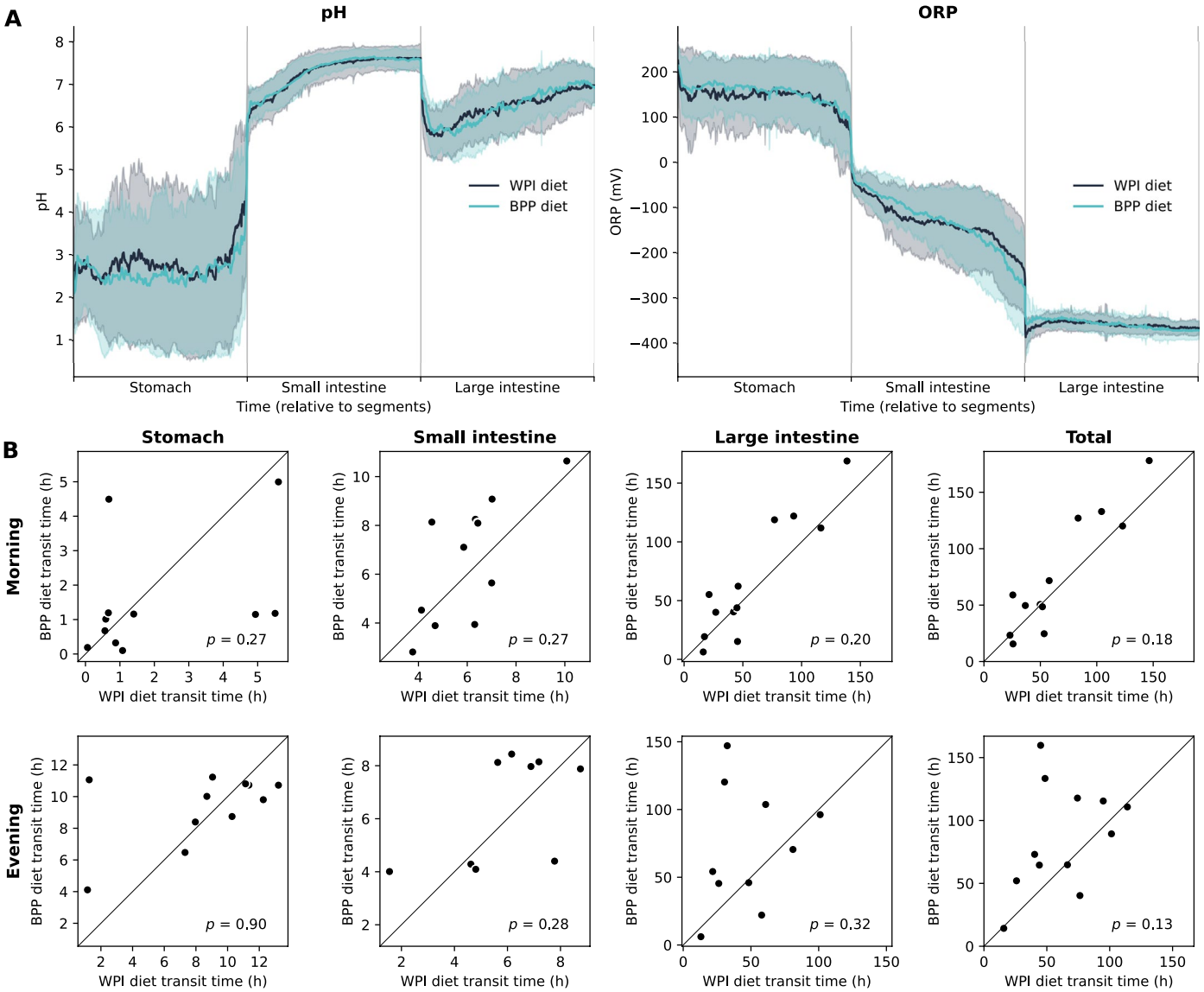

Extended Data Fig. 7 | No significant effect of dietary intervention on pH, ORP, or transit times. (**a**) Lines and shaded regions indicate the mean ± 1 s.d. of the (linearly rescaled) pH and ORP signals in the two different controlled diet conditions. Cluster-based permutation tests revealed no clusters of time points where a significant difference between these two diets could be observed: for the ORP data, the smallest (two-tailed) cluster *P*value was 0.33; for the pH data, no candidate clusters (contiguous sequences of time points which each exceed an individual, uncorrected *t*-test threshold of $p < 0.05$, two-tailed) were observed to begin with, nor did any individual time points from either sensor meet the Bonferroni-adjusted significance threshold (adjusted for the number of time points being compared). In short, we observed no significant effect of the dietary intervention on the pH or ORP measurements in any part of the GI tract. (**b**) Scatter plots of WPI-diet vs. BPP-diet transit times of the ingestible capsules through the stomach, small intestine, large intestine, and the whole gut, separated out for ingestibles taken in the morning and in the evening. Equality lines are plotted along the diagonal of each panel, such that points above the diagonal indicate capsules whose transit times were longer for the BPP diet than the WPI diet. Wilcoxon signed-rank tests revealed no significant effect of dietary intervention on any of these transit times (two-tailed *P*values reported in panels; smallest *P*value: $p = 0.13$, for the evening pills' whole-gut transit time).

https://doi.org/10.1038/s41928-025-01411-4

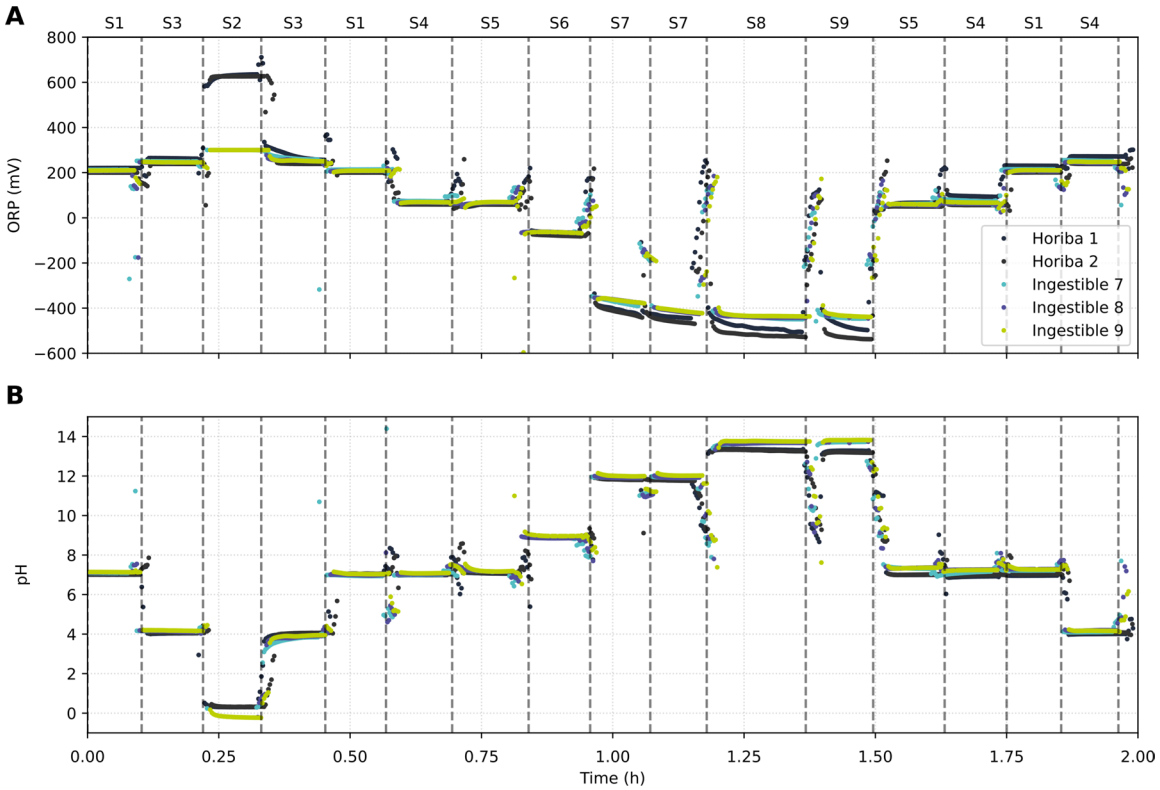

Extended Data Fig. 8 | In vitro validation of the GISMO sensors post-ingestion. Staircase measurement of ORP (**a**) and pH (**b**) profiles using three ingestibles post-ingestion retrieved from the participant of the clinical trial versus two commercial sensors (Horiba, Kyoto, Japan) in ORP (alternate) standards in the range of −550 mV to 600 mV with pH range between pH 0 and pH 14. The measurements were performed at body temperature (37 °C) within 2 h due to limited stability of ORP standard prepared in house by dissolving quinhydrone in pH buffers. The total transit times of these ingestibles were 46 h, 23 h, and 25 h.

https://doi.org/10.1038/s41928-025-01411-4

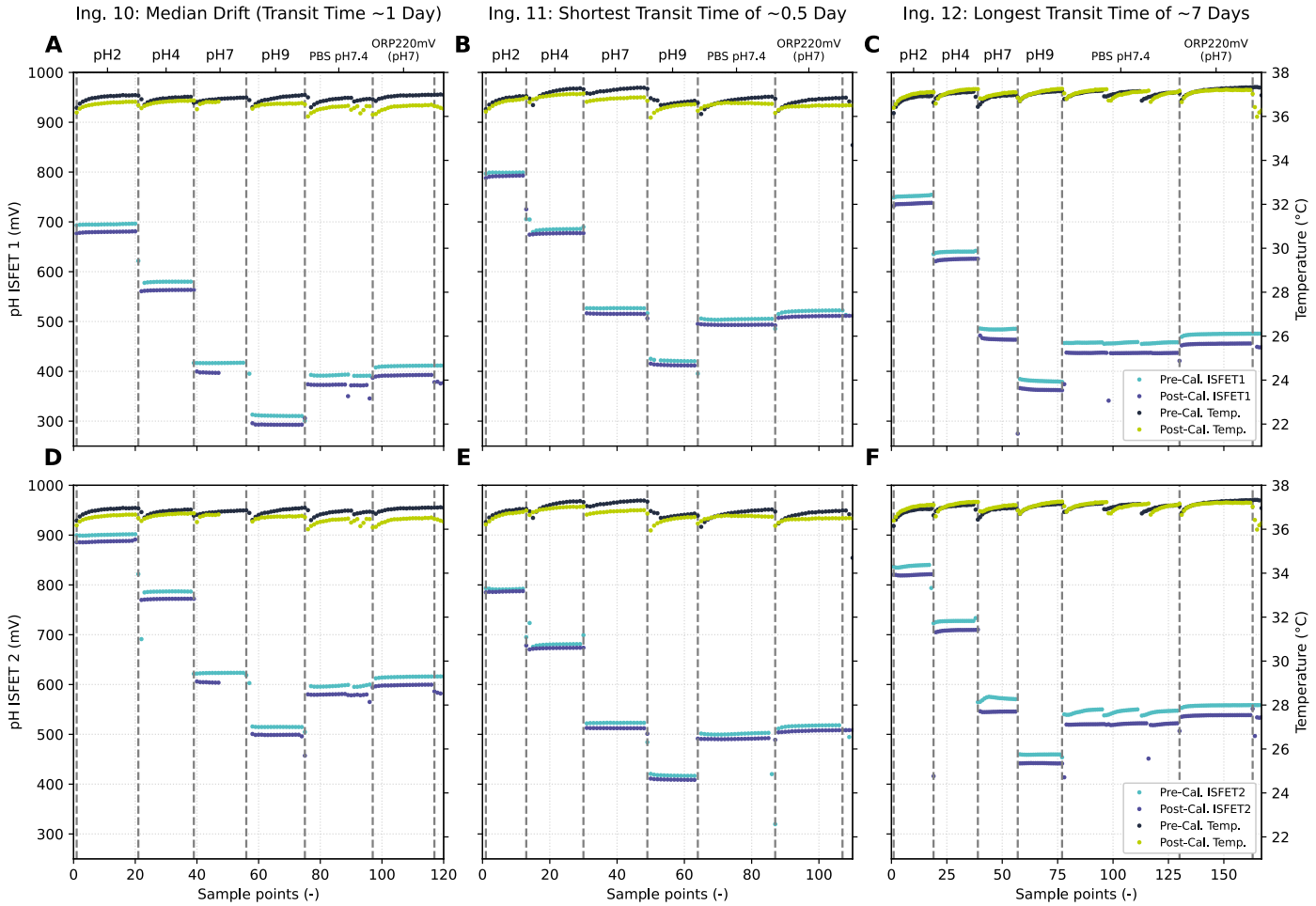

Extended Data Fig. 9 | Pre-ingestion calibration versus post-excretion calibration profiles of in total six pH ISFETs of three retrieved ingestibles with different transit times. (**a**) and (**d**) show ISFET1 and ISFET2 of a pill with a median drift profile (15.1 mV and 13.0 mV). (**b**) and (**e**) show the calibration of the pill with the shortest transit time (~0.5 day) with a drift of 5.1 mV and 3.0 mV; (**c**) and (**f**) show the same for an ingestible with the longest transit time of more than 7 days (12.9 mV and 17.6 mV drift).

nature portfolio

Corresponding author(s): Aniek Even

Last updated by author(s): Jun 2, 2025

Reporting Summary

Nature Portfolio wishes to improve the reproducibility of the work that we publish. This form provides structure for consistency and transparency in reporting. For further information on Nature Portfolio policies, see our Editorial Policies and the Editorial Policy Checklist.

Statistics

For all statistical analyses, confirm that the following items are present in the figure legend, table legend, main text, or Methods section.

n/a	Confirmed	
☐	☒	The exact sample size (*n*) for each experimental group/condition, given as a discrete number and unit of measurement
☐	☒	A statement on whether measurements were taken from distinct samples or whether the same sample was measured repeatedly
☐	☒	The statistical test(s) used AND whether they are one- or two-sided *Only common tests should be described solely by name; describe more complex techniques in the Methods section.*
☒	☐	A description of all covariates tested
☒	☐	A description of any assumptions or corrections, such as tests of normality and adjustment for multiple comparisons
☐	☒	A full description of the statistical parameters including central tendency (e.g. means) or other basic estimates (e.g. regression coefficient) AND variation (e.g. standard deviation) or associated estimates of uncertainty (e.g. confidence intervals)
☐	☒	For null hypothesis testing, the test statistic (e.g. *F*, *t*, *r*) with confidence intervals, effect sizes, degrees of freedom and *P* value noted *Give P values as exact values whenever suitable.*
☒	☐	For Bayesian analysis, information on the choice of priors and Markov chain Monte Carlo settings
☒	☐	For hierarchical and complex designs, identification of the appropriate level for tests and full reporting of outcomes
☐	☒	Estimates of effect sizes (e.g. Cohen's *d*, Pearson's *r*), indicating how they were calculated

Our web collection on statistics for biologists contains articles on many of the points above.

Software and code

Policy information about availability of computer code

Data collection	In-house developed firmware was developed for the ingestible and base devices. Also, an in-house developed computer application was developed for configuring data collecting settings and downloading of the data.
Data analysis	Data analysis was restricted to conventional and established methods, and implemented in Python (v. 3.12) scripts, making use of the "numpy" (v. 1.26), "scipy" (v. 1.14) and "pandas" (v. 2.2) packages (precise versions of these are not expected to materially influence the results).

For manuscripts utilizing custom algorithms or software that are central to the research but not yet described in published literature, software must be made available to editors and reviewers. We strongly encourage code deposition in a community repository (e.g. GitHub). See the Nature Portfolio guidelines for submitting code & software for further information.

Data

Policy information about availability of data

All manuscripts must include a data availability statement. This statement should provide the following information, where applicable:

- Accession codes, unique identifiers, or web links for publicly available datasets
- A description of any restrictions on data availability
- For clinical datasets or third party data, please ensure that the statement adheres to our policy

Access to underlying data, information on other study parameters and other types of subsets requires controlled access given the nature of the data falls under

special categories of personal data. Hence, processing of this data is subjected to specific provisions and requirements as set out in GDPR 2017/679. Restrictions related to existing data sharing agreements between concerning parties involved may apply. The data that supports the findings of this study can be made available upon request to the corresponding author within the limitations of the applicable regulations and ethical limitations. It is intended to respond to data requests within 3 months.

Human research participants

Policy information about studies involving human research participants and Sex and Gender in Research.

Reporting on sex and gender	Fifteen subjects, 8 women and 7 men, were included in the clinical trial. We attempted to have a balanced inclusion. Sex were self-declared.
Population characteristics	Inclusion criteria were age 16 years and older, body mass index (BMI) 18.5-30 kg/m2, regular bowel movement (at least one defecation per 48 hours), and suitable veins for cannula insertion. Exclusion criteria included, among others, (history of) gastrointestinal 45 diseases, history of major abdominal surgery, swallowing disorders, dysphagia to food or pills, implanted electromedical devices, using medication that can alter gastrointestinal motor function. Note one of the participants had a BMI above the inclusion criteria (30.9 kg/m2), for which a protocol deviation has been reported to the local medical ethics committee. The subjects, aged 52 ± 19 y (mean ± SD), were 176 ± 9 cm tall, with a body weight of 76.5 ± 13.3 kg, and BMI of 24.6 ± 3.1 kg/m2.
Recruitment	Subjects were recruited via a volunteer database of the Human Research Unit of Wageningen University & Research. The selection procedure might have induced some bias, since the database includes research-minded volunteers, with a potentially similar background, though we did observe a wide range in age. We only included people with a good understanding of the Dutch language, which might also have introduced a bias. Since this study was only a first pilot in healthy volunteers, we did not aim to get a representative sample of the whole population. The subjects were self-declared healthy volunteers. For the interpretation of the ORP baseline values it's good to realize that 'healthy' can be a subjective term.
Ethics oversight	Medical ethical committee of the East region of The Netherlands (NL84483.091.23)

Note that full information on the approval of the study protocol must also be provided in the manuscript.

Field-specific reporting

Please select the one below that is the best fit for your research. If you are not sure, read the appropriate sections before making your selection.

☒ Life sciences ☐ Behavioural & social sciences ☐ Ecological, evolutionary & environmental sciences

For a reference copy of the document with all sections, see nature.com/documents/nr-reporting-summary-flat.pdf

Life sciences study design

All studies must disclose on these points even when the disclosure is negative.

Sample size	No sample size calculations could be performed because this is the first time redox balance measurements have been performed in human. The human trial was considered an exploratory study which focussed on both the feasibility of the ingestible as on a dietary intervention with contrasts in protein digestibility. A total of 15 participants were included in the study. As the overall aim of the trial was to study the effect of dietary protein sources on protein fermentation, the sample size was based on this. However, a solid power calculation was not possible as there is also limited information in literature about the relation between protein digestibility and protein fermentation related metabolites. But there are multiple studies that focused on the effect of increased dietary protein intake on protein fermentation by measuring protein fermentation related metabolites in urine or feces of 4-17 subjects per treatment [1-4]. We chose to perform the study with a number of participants in the upper range of these aforementioned studies: n=15. A power analysis for the ingestibles ORP sensor would also not have been possible since this is the first time redox balance is measured in the human GI tract. The study was designed as a cross-over clinical trial design to increase statistical power even with a relatively low number of participants, because participants act as their own control. 1. Cummings, J. H., Hill, M. J., Bone, E. S., Branch, W. J. & Jenkins, D. J. The effect of meat protein and dietary fiber on colonic function and metabolism II. Bacterial metabolites in feces and urine. Am J Clin Nutr 32, 2094–2101 (1979). 2. Geypens, B. et al. Influence of dietary protein supplements on the formation of bacterial metabolites in the colon. Gut 41, 70–76 (1997). 3. Magee, E. A., Curno, R., Edmond, L. M. & Cummings, J. H. Contribution of dietary protein and inorganic sulfur to urinary sulfate: toward a biomarker of inorganic sulfur intake. Am J Clin Nutr 80, 137–142 (2004). 4. Russell, W. R. et al. High-protein, reduced-carbohydrate weight-loss diets promote metabolite profiles likely to be detrimental to colonic health. Am J Clin Nutr 93, 1062–1072 (2011).

Data exclusions	Data that were deemed to be faulty or untrustworthy were excluded from further analysis, based on the following criteria. For one ingestible, one of the two pH sensors failed the pre-study calibration acceptance criteria, and thus data from this one pH sensor was not analyzed. Out of 69 ingestibles, three ingestibles were completely removed from analysis, leaving 66 remaining for evaluation. One subject became ill and experienced GI symptoms during the second dietary intervention, and therefore data from this period (two ingestibles), which would not be representative of normal healthy gut conditions, were excluded. One ingestible had a premature shutdown due to battery failure in the stomach; this ingestible was removed because we did not have a complete GI segment. For another nine ingestibles — two other ingestibles with premature shutdown due to battery failure, one in the small intestine and one in the large intestine, and seven ingestibles with unexpectedly long transit times that entered into ultra-low-power mode before excretion, resulting in incomplete coverage of some GI segments — only segments were analyzed for which a beginning and end could be identified, and segment summary statistics were only computed if the ingestible had completed at least 80% of its transit time through a segment before pill shutdown. Finally, data points were excluded from analysis if they were too near, or exceeded the limits of the electronics, or in case of very abrupt and intense fluctuations in the measurements that were deemed unlikely to be physiological in origin. On average, 0.7% of measurements were excluded per ingestible, with a maximum of 12.16% (not including cases where entire ingestibles, sensors or segments were excluded).
Replication	This is an explorative study, showing the first-in-human data of redox balance in human. We did not aim to replicate the data. Follow-up studies will be needed to replicate the data and show the role of redox balance in patient groups (as described in the clinical impact and applications section). The in-vitro validation was preformed with multiple ingetibles (2x 3 ingestibles), showing good agreement between sensors (Fig 3). Performance test on the reference electrodes were performed on 10 referlence electrodes, showing good agreement (Extended Data Fig 1). Power profiles and operations times were tested in dublicate. Showing very similar behavior (Exteneded Data Fig 3).
Randomization	The participants in the study received two different protein sources in a cross-over dietary controlled trial. The order of the protein sources was randomized.
Blinding	Participants were blinded to the used protein source, investigators were not blinded. We did report on the difference in ORP between the 2 diets, but this was not the main objective of this study, it was only an additional analysis. That is why blinding was not deemed necessary for that specific analysis.

Reporting for specific materials, systems and methods

We require information from authors about some types of materials, experimental systems and methods used in many studies. Here, indicate whether each material, system or method listed is relevant to your study. If you are not sure if a list item applies to your research, read the appropriate section before selecting a response.

Materials & experimental systems

n/a	Involved in the study
☒	☐ Antibodies
☒	☐ Eukaryotic cell lines
☒	☐ Palaeontology and archaeology
☐	☒ Animals and other organisms
☐	☒ Clinical data
☒	☐ Dual use research of concern

Methods

n/a	Involved in the study
☒	☐ ChIP-seq
☒	☐ Flow cytometry
☒	☐ MRI-based neuroimaging

Animals and other research organisms

Policy information about studies involving animals; ARRIVE guidelines recommended for reporting animal research, and Sex and Gender in Research

Laboratory animals	Seven gilts (Landrace/Large White), with average body weight of 23.4 kg. Around 10 weeks old.
Wild animals	Study did not involve wild animals.
Reporting on sex	Only female pigs were used due to availability. Sex was not considered in the study designs. Results are applicable for for both sexes, although individual variation needs to be taken into account.
Field-collected samples	The 7 pigs, were housed in pairs of 2 or 3 on straw. Room temperature was maintained at 21 degree Celsius with a 12h light/dark cycle, switching at 7:00 and 19:00. Pens were cleaned daily. Animals had ad libitum access to water.
Ethics oversight	The experimental protocol was approved by the Animal Welfare Officer of Wageningen University and Research.

Note that full information on the approval of the study protocol must also be provided in the manuscript.

Clinical data

Policy information about clinical studies

All manuscripts should comply with the ICMJE guidelines for publication of clinical research and a completed CONSORT checklist must be included with all submissions.

Clinical trial registration	NCT06161155
Study protocol	The study overview, objectives, study population, and study design can be found on clinicaltrials.gov. https://clinicaltrials.gov/study/NCT06161155
Data collection	Study start: 2023-11-21; study completion 2024-02-07. Ingestion of the ingestible devices was done at the Human Research Unit at Wageningen University & Research. Data collection started there. People were allowed to go home and continue their normal routines after. Data collection finished after the exit of the ingestibles were confirmed.
Outcomes	The objectives of the study were: Primary Objective(s): • To investigate the feasibility of the GISMO GEN1 System to monitor biomarkers in the gastrointestinal tract by studying the ingestible transit time, data coverage, participant experience, and serious adverse events (if applicable). • To investigate the effect of a 7-day high versus low digestible protein source present in the diet on protein fermentation in healthy subjects, measured by ammonia concentrations. Ammonia will be measured in feces, urine, and with the ingestible. Secondary Objective(s): • To correlate protein fermentation related metabolites between feces, urine, blood, and the GISMO GEN1 ingestible. • To investigate the effect of protein fermentation on pH profiles in the gastrointestinal tract measured by the GISMO GEN1 ingestible. • To investigate the effect of a 7-day high versus low digestible protein on microbiome composition in feces. • To investigate the correlations between protein fermentation related metabolites and gastrointestinal transit time. • To compare absorption kinetics of amino acids and protein fermentation metabolites in blood between a high versus low digestible protein diet. For the primary objective, we proved the feasibility of the GISMO GEN1 system. The mean transit time of the ingestibles was 67.5 (SD 7.2) hours. Overall data coverage (i.e., percentage of correctly received data packets) was 90.3% (range 59.1-98.9% across all ingestibles). Participants confirmed the ease of use and confirmed that they were wiling to take another ingestible. There were no device related adverse events. The other objectives were all designed to study protein fermentation. This is not relevant for the data presented in this manuscript. There is no direct hypothesized relationship between the ORP sensor and protein fermentation.